Towards a new model for kimberlite petrogenesis: Evidence from unaltered kimberlites and mantle minerals

Vadim S. Kamenetsky [a,*], Alexander V. Golovin [b,c], Roland Maas [d], Andrea Giuliani [d], Maya B. Kamenetsky [a], Yakov Weiss [e]

[a] School of Physical Sciences, University of Tasmania, Hobart, Tasmania 7001, Australia
[b] V.S. Sobolev Institute of Geology and Mineralogy, Siberian Branch, Russian Academy of Science, Prosp. Ak. Koptyuga 3, 630090 Novosibirsk, Russia
[c] Novosibirsk State University, Novosibirsk 630090, Russia
[d] School of Earth Sciences, University of Melbourne, Parkville, 3010 Victoria, Australia
[e] Lamont-Doherty Earth Observatory, Columbia University, Palisades, NY 10964, USA

A B S T R A C T

Kimberlites represent magmas derived from great mantle depths and are the principal source of diamonds. Kimberlites and their xenolith cargo have been extremely useful for determining the chemical composition, melting regime and evolution of the subcontinental mantle. The late-Devonian Udachnaya (means *Fortuitous*) pipe hosts the largest diamond deposit in Russia (>60% diamond quantity and value) and one of the largest in the world, supplying gem-quality diamonds (~12% of world production). Since its discovery in 1956, the Udachnaya kimberlite pipe has become a "type locality" for geochemists and petrologists studying mantle rocks and mantle physical–chemical conditions. Apart from hosting a diverse suite of extremely well-preserved mantle xenoliths, the host kimberlite (East body) is the only known occurrence of fresh kimberlite, with secondary serpentine almost absent and uniquely high Na_2O and Cl (up to 6.2 wt.%) and low H_2O (<1 wt.%) contents. The discovery of such compositional features in the only unaltered kimberlite has profound implications for models of parental kimberlite magma compositions, and the significance of the high Na and Cl abundances in the Udachnaya-East pipe has therefore been subjected to vigorous criticism. The main argument against a primary magmatic origin of high Na-Cl levels involves the possibility of contamination by salt-rich sedimentary rocks known in the subsurface of the Siberian platform, either by assimilation into the parental magma or by post-intrusion reaction with saline groundwaters.

In this paper we review evidence against crustal contamination of Udachnaya-East kimberlite magma. This evidence indicates that the kimberlitic magma was not contaminated in the crust, and the serpentine-free varieties of this kimberlite owe their petrochemical and mineralogical characteristics to a lack of interaction with syn- and post-magmatic aqueous fluids. The groundmass assemblage of this kimberlite, as well as earlier-formed melt inclusions, contains alkali carbonate, chloride and other Na- and Cl-bearing minerals. This mineralogy reflects enrichment of the parental melt in carbonate, chlorine and sodium. The combination of low H_2O, high alkali-Cl abundances, lack of serpentine, and the presence of alteration-free mantle xenoliths all indicate that the Udachnaya-East kimberlite preserves pristine compositions in both kimberlite and mantle xenoliths. Evidence for broadly similar chemical signatures is found in melt inclusions from kimberlites in other cratons (South Africa, Canada and Greenland in our study). We demonstrate that two supposedly "classic" characteristics of kimberlitic magmas – low sodium and high water contents – relate to postmagmatic alteration.

A "salty" carbonate composition of the kimberlite parental melt can account for trace element signatures consistent with low degrees of partial melting, low temperatures of crystallisation and exceptional rheological properties that enable kimberlite magmas to rise with high ascent velocities, while carrying a large cargo of entrained xenoliths and crystals. Our empirical studies are now supported by experimental data which suggest that carbonate-chloride fluids and melts derived by liquid immiscibility are a crucial factor of diamond formation.

* Corresponding author. Tel./fax: +61 3 62267649.
E-mail addresses: Dima.Kamenetsky@utas.edu.au (V.S. Kamenetsky), avg@igm.nsc.ru (A.V. Golovin), maasr@unimelb.edu.au (R. Maas), a.giuliani@student.unimelb.edu.au (A. Giuliani), Maya.Kamenetsky@utas.edu.au (M.B. Kamenetsky), yakov.weiss@mail.huji.ac.il (Y. Weiss).

Contents

1. Introduction

Although occurrences of kimberlite are rare and of small volume, the unusually deep-seated mantle sources of kimberlite magmas and the association with diamonds and mantle xenoliths has long generated a disproportionate interest in the scientific and exploration communities. Significant effort has gone into characterising styles of emplacement, ages, petrography, mineralogy, textural and compositional characteristics, and the tectonic setting of kimberlites. However, a full understanding of kimberlite petrogenesis has been hampered by effects of pre-emplacement contamination, syn-emplacement stratification and syn/post-emplacement alteration of kimberlite rocks, all of which tend to hinder recognition of primary/parental kimberlite magma compositions. The prevailing practice of using bulk kimberlite compositions to derive parental compositions has been challenged by research on exceptionally fresh kimberlite specimens from the Devonian Udachnaya-East pipe (Kamenetsky et al., 2004; Kamenetsky et al., 2007a; Kamenetsky et al., 2009c; Kamenetsky et al., 2012b) and other relatively fresh kimberlites (Kamenetsky et al., 2009b; Kamenetsky et al., 2013), detailed mineralogical studies and related mass-balance calculations (e.g., Brett et al., 2009; Patterson et al., 2009; Pilbeam et al., 2013) and thoughtfully designed experiments (e.g., Sparks et al., 2009; Brooker et al., 2011). A review of existing data and interpretations, combined with new results and ideas, is presented in this paper.

2. Udachnaya-East kimberlite: common and unique properties

2.1. Location, host rocks and petrography

The Udachnaya diamondiferous kimberlite pipe is located in the northwestern part of the Daldyn–Alakit kimberlite province in Siberia (Fig. 1). At the surface, two adjacent kimberlite bodies (East and West) are recognised, and these can be traced to separate pipes in underground workings beyond ~250–270 m. Based on stratigraphic relationships both intrusions formed near the Devonian–Carboniferous boundary (~350 Ma), and radiometric age estimates vary from 389

to 335 Ma (Maslovskaja et al., 1983; Burgess et al., 1992; Maas et al., 2005). The most robust age constraints suggest kimberlite emplacement at ~367 Ma, based on perovskite U–Pb and phlogopite RbSr dates presented by Kinny et al. (1997) and Kamenetsky et al. (2009c).

The Udachnaya pipes are emplaced within thick (up to 2.5 km) terrigenous-carbonate and carbonate rocks along the western flank of the Olenek artesian basin (Fig. 1 in Pavlov et al., 1985; Fig. 1 in Alexeev et al., 2007). The stratigraphy of the sedimentary cover around the pipes is well known from >30 exploration holes to 700–1700 m depth, and from three geotechnical holes (KCC-1,2,3 to 1100–1500 m) drilled adjacent to the pipe, ~800–1000 m south from the open pit (Fig. 1B). Furthermore, a complete stratigraphic record of this part of the Daldyn–Alakit kimberlite province was recovered in two deep holes which intersected crystalline basement at ~2500 m. These deep drillholes (#703 and # 2531, Figs. 1B, 2) are located 1.5 km to the southeast and 4 km to the northeast from the pipe and recovered limestones, dolomites, siltstones, mudstones and sandstones (Fig. 2B).

The eastern and western bodies of the Udachnaya kimberlite pipe differ in terms of mineralogy, petrography, composition, and degree of alteration. While alteration in the western pipe is typical of kimberlites globally, alteration within the Udachnaya-East pipe is much weaker, and parts of this pipe are unique in showing no serpentinisation of olivine and groundmass. The occurrence of "unaltered kimberlite" in the Udachnaya-East (UE) pipe (Figs. 1A, 3D, E, 4) was first reported by Marshintsev et al. (1976), followed by more detailed descriptions a decade later (Marshintsev, 1986). In these reports, "unaltered kimberlite", intersected by drilling at depths below 350 m, is described as a dense, dark-grey rock with olivine unaffected by serpentinisation, unusually low H$_2$O$^+$ (1.95 wt.%) and relatively high Na$_2$O (0.52 wt.%), compared to the dominant serpentinised kimberlites in the pipe. Marshintsev's "unaltered kimberlites" were subsequently studied by other Russian researchers (e.g., Kornilova et al., 1981; Egorov, 1986; Egorov et al., 1986, 1988; Sobolev et al., 1989; Egorov et al., 1991; Kharkiv et al., 1991) but failed to gain attention outside the former USSR.

Information on weakly altered and unaltered UE kimberlites published prior to early 2000s is difficult to relate to any specific rock type

in the pipe. These rocks, referred to as the *Serpentine Free Udachnaya East* (SFUE) kimberlite (Kopylova et al., 2013; Kostrovitsky et al., 2013), neither represent a distinct petrographic type, nor do they belong to a single emplacement event. Their major feature is unaltered olivine, even in the kimberlite varieties containing abundant sedimentary xenoliths (>25 vol.%), whereas serpentine is not totally absent in the groundmass of some samples (Marshintsev, 1986; Egorov et al., 1991; Kharkiv et al., 1991).

From 2003–2013, one of us (AVG) methodically documented different types of UE kimberlites containing unaltered olivine recovered from 420–620 m depth. Using the kimberlite classification scheme of Clement and Skinner (1985) two major rock types could be distinguished: kimberlite breccia (KB) and kimberlite (K), which differ based on clast content (>15 and <15 vol.%, respectively). Kimberlite breccia (KB) can be further classified based on the content of sedimentary fragments (from ≥ 50 vol.% in KB-1 to 15–20 vol.% in KB-4) and degree of preservation of olivine and mantle xenoliths (Fig. 3A, B). Type KB-4 is the least serpentinised (i.e., most olivine is unaltered and serpentine is sporadic) although chloride and alkali carbonate minerals are absent in the groundmass. All types of KB contain veins filled with hydrothermal gypsum.

Kimberlite (K) with ≤ 6 vol.% of sedimentary xenoliths occurs within a subvertical, 30–50 m wide body surrounded by the kimberlite breccia (KB-3 and KB-4) in the central part of the pipe below 400 m depth (Figs. 1A, 3C, D). One subtype, K-1, does not contain serpentine in either groundmass or as an alteration product of olivine, which is reflected in low H_2O content (<1 wt.%). K-1 kimberlites are further characterised by the presence of alkali carbonate and chloride minerals in the groundmass, and by excellent preservation of mantle xenoliths (e.g., Doucet et al., 2012; Agashev et al., 2013; Doucet et al., 2013). It appears that the serpentine-free kimberlite has never been affected by postmagmatic low-temperature processes which elsewhere, for example in the kimberlite breccia (KB) facies, resulted in deposition of gypsum in fractures and cavities. A special feature of the unaltered kimberlite is the presence of angular to rounded "nodules" rich in chlorides and intergrown alkali carbonates and chlorides (Figs. 3D, 4; also see Figs. 2A–C in Kamenetsky et al., 2007a, Figs. 1A–D in Kamenetsky et al., 2007b). The borders of these "nodules" appear to be unaffected by chemical reactions (e.g., dissolution and melting) with the enclosing kimberlite.

Another kimberlite subtype, K-2 (Fig. 3C), comprises largely unaltered olivine but contains serpentine in the groundmass; this is reflected in higher bulk rock H_2O contents (up to 4.5 wt.%) compared to serpentine-free facies K-1 (Kamenetsky et al., 2012b). Alkali carbonates and chlorides are absent in this kimberlite type and the contents of Na_2O and Cl (<1 wt.%) are significantly reduced compared to those in K-1. Sections of the pipe composed of facies K-1 and K-2 contain vein-like domains up to 20 cm thick of kimberlite which is essentially free (≤1 vol.%) of sedimentary xenoliths (Fig. 3E). These domains have distinct contacts with the host rock, contain unaltered olivine crystals aligned along the vein strike, and carry abundant alkali carbonate and chloride minerals in the groundmass. This kimberlite variety is interpreted as a late intrusive phase.

2.2. Mineralogy and petrochemistry

UE K-1 facies kimberlites are olivine-rich (Fig. 1 in Kamenetsky et al., 2012b, Figs. 2, 6 in Kamenetsky et al., 2008), Fig. 2 in Kamenetsky et al., 2009b), a feature shared by the majority of hypabyssal kimberlites, excluding very rare aphanitic kimberlites, such as those from Kimberley, Benfontein and Premier in South Africa (Shee, 1985; le Roex et al., 2003) and Jericho, Canada (Price et al., 2000). The large abundance of olivine (45–60 vol.%) is reflected in high MgO contents of bulk rock analyses (28–36 wt.%). Two populations of olivine can be recognised based on size, morphology, and entrapped inclusions. Consistent with many other studies of kimberlitic olivine (e.g., Mitchell, 1973; Boyd and Clement, 1977; Mitchell, 1978; Sobolev et al., 1989; Nielsen and

Jensen, 2005) the populations are represented by olivine-I (interpreted by different workers as cognate phenocrysts or xenocrysts) and groundmass olivine-II. Recent studies indicate that both populations significantly overlap in terms of composition and possibly origin (e.g., Kamenetsky et al., 2008; Brett et al., 2009; Arndt et al., 2010). Olivine is set in a matrix of carbonates (calcite, shortite $Na_2Ca_2(CO_3)_3$ and K-bearing alkali-carbonate $(Na, K)_2Ca(CO_3)_2)$, chlorides (halite and sylvite), minor Na-K sulphates, phlogopite, sodalite $(Na_8Al_6Si_6O_{24}Cl_2)$, apatite and opaque minerals (e.g., spinel group minerals, perovskite, Fe ± (Ni,Cu,K) sulphides, including djerfisherite $K_6Na(Fe,Cu,Ni)_{25}S_{26}Cl$ and rasvumite KFe_2S_3) (Kamenetsky et al., 2004, 2007a; Sharygin et al., 2008; Kamenetsky et al., 2012b); monticellite is occasionally present in K-1. Textural relationships are illustrated in Fig. 5 (also see Fig. 1 in Kamenetsky et al., 2004, Fig. 2 in Kamenetsky et al., 2012b).

Bulk rock compositions of UE kimberlites are characterised by high CaO (8.1–18.2 wt.%) and CO_2 (4.1–14.1 wt.%) and low Al_2O_3 (1.1–2.3 wt.%) contents. Trace element compositions are similar to those of other kimberlites, with high concentrations of highly incompatible elements and depletion in heavy rare-earth elements and yttrium (Kamenetsky et al., 2012b). The overall petrographic, mineralogical and chemical characteristics (including radiogenic isotopes, see below) of the UE kimberlites suggest that they belong to archetypal

Fig. 1. A. Open mine pit of the Udachnaya kimberlite pipe and approximate locations of the Udachnaya-East and unaltered kimberlite body (photo taken in 2008, 560 m depth of the pit). B. Exploration (KCC-1, 2, 3) and parametric drill holes (#703 and #2531) in vicinity of the Udachnaya mine pit. The stratigraphic column in the drill hole #703 is shown on Fig. 2B.
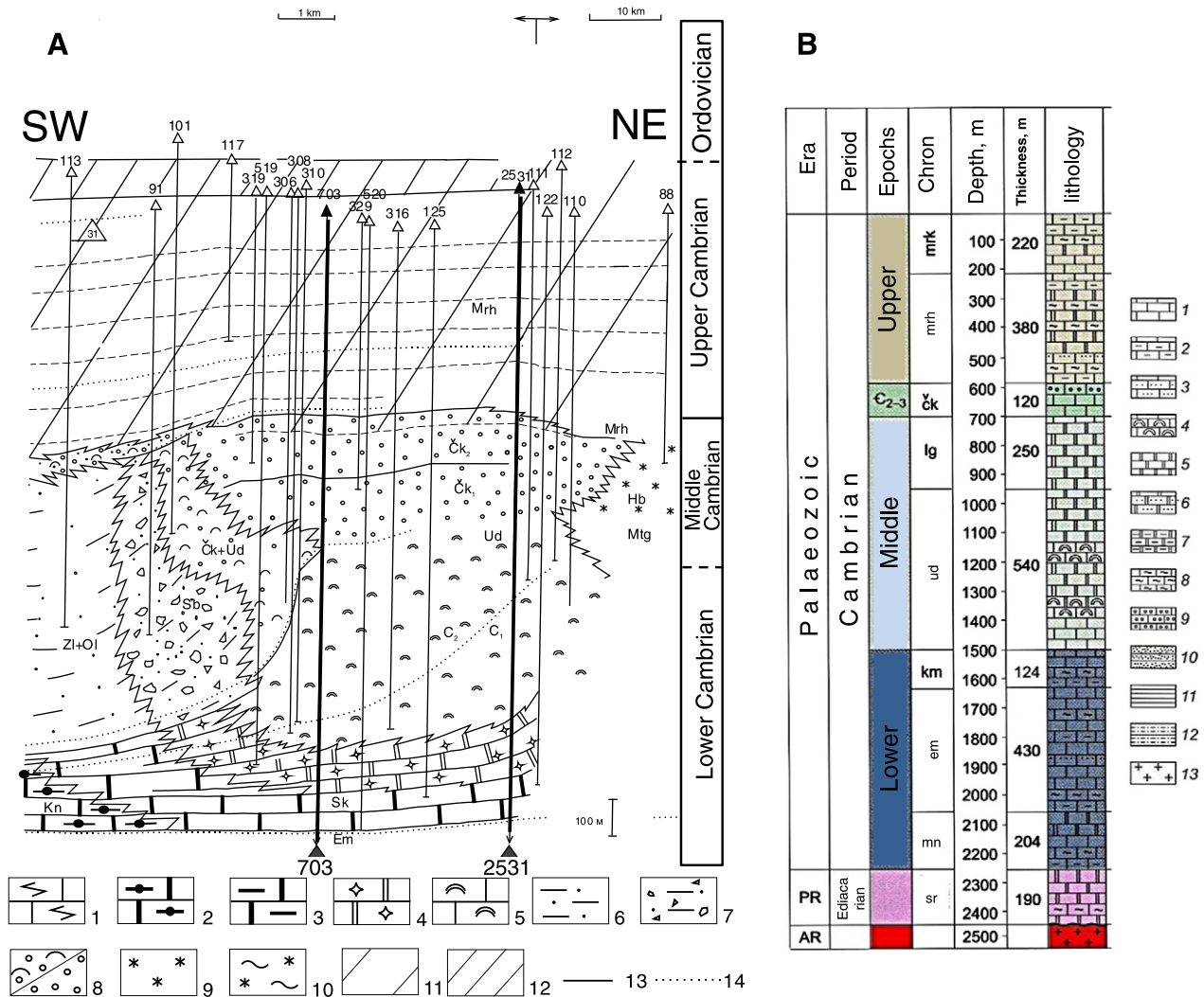
Fig. 2. Cross-section of the sedimentary sequence in the region of the Udachnaya-East pipe and position of parametric drill holes #703 and #2531 (A) and detailed stratigraphic column through the parametric hole #703 (B) after (Sukhov and Lobanov, 2003; Drozdov et al., 2008; Alexseev, 2009). The sedimentary sequence (A) is represented by red wackestones with limestone lithoclasts (1), black bituminous silty limestone, mudstone and marl (2), brown bituminous silty limestone and marl (3), detrital cavernous dolomite (4), reef detrital-granular, variably dolomitised limestone (5), dark-grey and green silty limestone and marl (6), dark-grey and green detrital limestone, mudstone and breccia (7), light-coloured ooidal limestone and cavernous dolomite with sparry calcite and halite in pores (8, Chukuckskaya suite), red carbonated siltstone, claystone, dolomite and mudstone with gypsum nodules, interbedded (often rhythmically) with detrital-clastic limestone and dolomite (9, 10), interbedded grey marl and sedimentary breccia comprising stromatolite limestone and dolomite, sometimes with mudstones (11), dolomitised siltstone and marl (12). Boundaries of stratigraphic units (13), biostratigraphic markers (14) and drill holes (triangles) are also shown. The sedimentary sequence (B) is represented by limestones (1 — clear, 2 — silty, 3 — sandy, 4 — organogenic), dolomites (5 — clear, 6 — sandy, 7 — silty), marls (8), calcareous conglomerates (9), sandstones (10), mudstones (11), siltstones (12) and crystalline basement (13). The main stratigraphic units are: Morkokinskaya (mrk), Markhinskaya (mkh), Chukuckskaya (čk), lagoon–sabkh (lg), Udachninskaya (ud), Kuonamskaya (km), Emyaksinskaya (em). Location of the Udachnaya-East pipe relative to parametric drill holes #703 and #2531 is shown on Fig. 1B.

(Mitchell, 1995) or group-I (Smith, 1983; Clement and Skinner, 1985) kimberlite. However, the high abundances of Na$_2$O and Cl (up to 6 wt.%) and S (up to 0.3 wt.%), coupled with low H$_2$O (<1 wt.%), in UE kimberlites (type K-1) are unique among kimberlites studied to date (see Figs. 6, 7 in Kamenetsky et al., 2012b). High Na and Cl, and low H$_2$O reflect the presence of abundant groundmass alkali carbonate and halide minerals, and an absence of serpentine, respectively. Preservation of primary magmatic water-soluble minerals in UE kimberlite has been interpreted (by us and by others, e.g., Egorov et al., 1991) to reflect initial low H$_2$O contents in the parental kimberlite magma; low initial magma water content would have minimised alteration of early formed minerals by magmatic fluids.

2.3. Inclusions in olivine

Three main types of inclusions are recognised in UE olivine: crystal, fluid and melt (Golovin et al., 2003; Kamenetsky et al., 2004; Golovin et al., 2007; Kamenetsky et al., 2008, 2009a,b; Kamenetsky and Kamenetsky, 2010). The distribution of inclusions (<1 to ~400 μm) within single olivine grains can be very heterogeneous, with some parts totally devoid of inclusions and other parts almost opaque because of abundant inclusions. Crystal inclusions belong to mantle (low- and high-Ca pyroxene, garnet, picroilmenite, sulphide) and magmatic (rutile, perovskite, phlogopite, Cr-spinel, olivine) assemblages, although some overlap in origin (i.e. high- vs low-pressure) cannot be excluded. Inclusions of melt and fluid are always restricted to healed fractures (Fig. 2 in Kamenetsky et al., 2004, Fig. 4 in Kamenetsky et al., 2008, Fig. 5 in Kamenetsky et al., 2009b), but they predate crystallisation of the olivine-II outermost rims (Kamenetsky et al., 2008). Melt inclusions in olivine are predominantly alkali carbonate-chloride in composition (Golovin et al., 2003; Kamenetsky et al., 2004; Golovin et al., 2007; Kamenetsky et al., 2009b), whereas typical silicate melt inclusions have not been recorded to date. Noteworthy, inclusions of mantle-derived Cr-diopside in olivine-I are often associated with the carbonate-chloride material, which forms
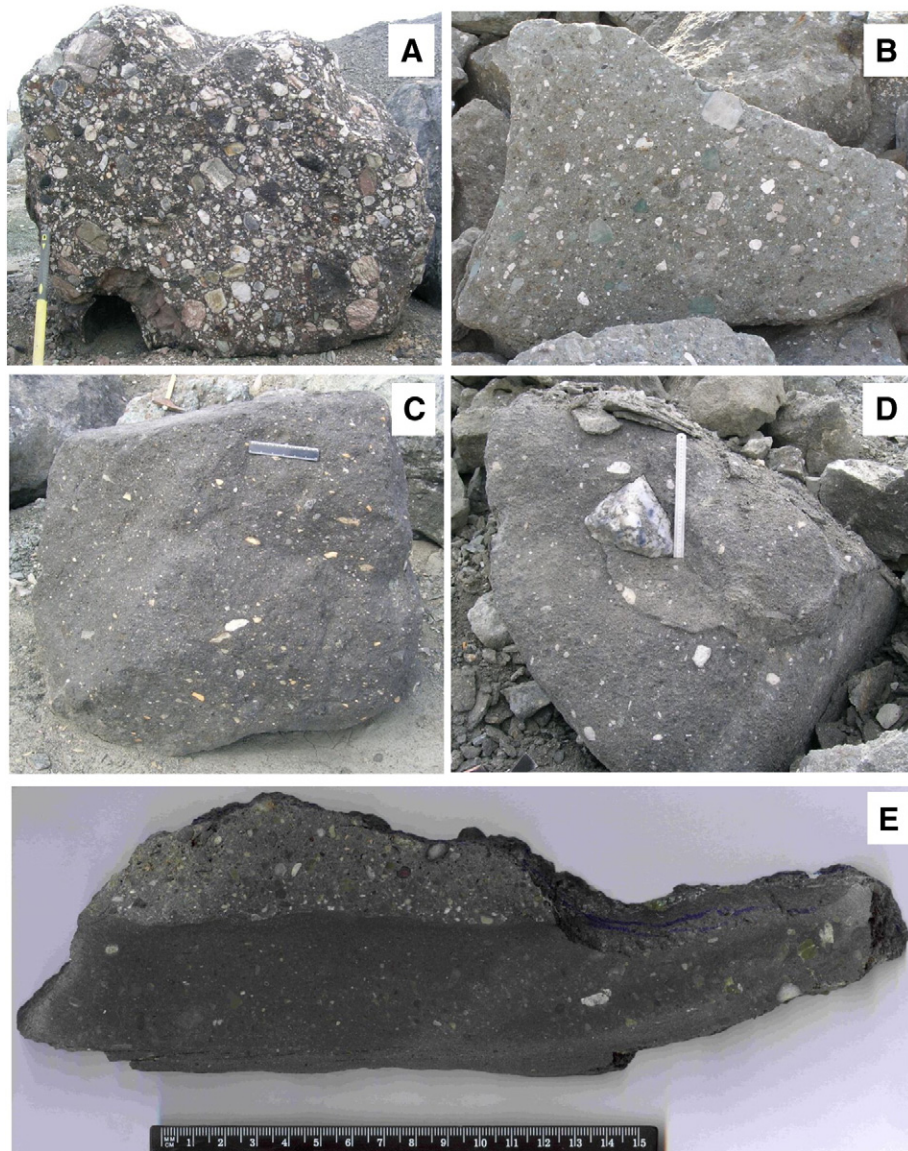
Fig. 3. Petrographic and textural types of the UE kimberlites. A, B kimberlite breccia KB-1 and KB-4; C, D kimberlite K-2 and K-1, respectively (close-up on Fig. 4G); E — a vein-like kimberlite in K-1.

coatings on surfaces and inclusions inside clinopyroxene grains (Figs. 2, 3 in Kamenetsky et al., 2009a).

Many melt inclusions are interconnected by thin channels, which suggests that "necking down" can explain variable proportions of fluid and mineral phases in neighbouring inclusions. The crystallised assemblage in the melt inclusions, represented by Na–K–Ca carbonates (shortite, nyerereite, northupite), halite, sylvite, phlogopite-tetraferriphlogopite, calcite, Fe–Ti–Cr oxides, aphthitalite, djerfisherite and olivine (Golovin et al., 2003; Kamenetsky et al., 2004; Golovin et al., 2007), closely resembles the phase composition of the K-1 groundmass. The melt inclusions homogenise at 660–760 °C (Fig. 6) during heating stage experiments at 1 atm. During cooling the melt undergoes immiscibility with development of carbonate- and chloride-rich conjugate liquids at 610–580 °C and solidifies at 200–160 °C (Fig. 6). These experiments further confirm the high-temperature origin and essentially non-silicate composition of the entrapped liquids.

2.4. Chloride-carbonate "nodules"

The chloride-carbonate "nodules" characteristic of unaltered kimberlite facies K-1 are usually 5 to 30 cm across, have rounded to angular shapes and preserve sharp contacts with the host kimberlite (Fig. 4; also Fig. 2 in Kamenetsky et al., 2007a). Alkali carbonate and chloride minerals of the type found in the UE kimberlite groundmass are dominant minerals in the nodules. The chloride assemblage is dominated by halite, whereas individual crystals of sylvite are rare. However, sylvite is included in halite as round grains and irregular, bleb-like formations, resembling emulsion textures (Fig. 3 in Kamenetsky et al., 2007a; also see experimental data on immiscible halide liquids in Mitchell and Kjarsgaard, 2008), and can make up to 30 vol.% of total chlorides. Sylvite is characterised by heterogeneous and very high contents of bromine (up to 8 wt.%), by far exceeding common abundances of Br in evaporite salt minerals (<0.4%; Holser, 1979). Carbonates are present as 1–5 mm thick sheets set in a fine-grained mass of chlorides (Fig. 6H; also Figs. 2A–C in Kamenetsky et al., 2007a). The regular alignment of the carbonate sheets within a chloride matrix is reminiscent of the spinifex-like textures observed in olivine-hosted melt inclusions undergoing chloride-carbonate liquid immiscibility at ~600 °C (Fig. 6G).

The carbonate assemblage within the nodules is dominated by anhydrous and hydrated Na–Ca carbonates with variable Ca/Na ratios and highly variable amount of K_2O and SO_3 (both up to 14 wt.%), whereas calcite is subordinate. The alkali sulphates, aphthitalite (($Na_{0.25}$ $K_{0.75}$)
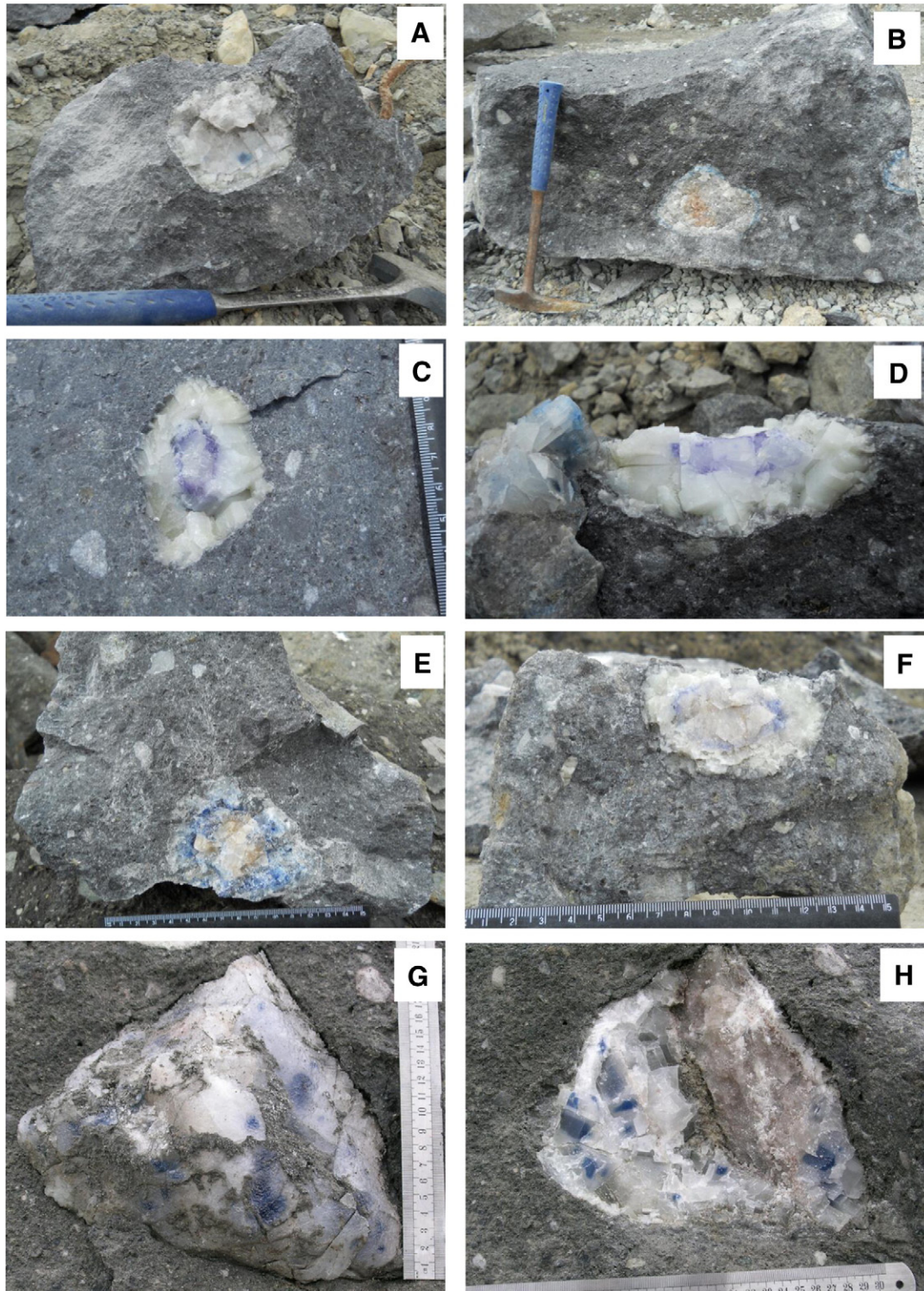
Fig. 4. Carbonate-chloride nodules (segregations) in kimberlite (K-1). Photos A–F were taken immediately after rock boulders were split and nodules appeared on surfaces. Note spotty and concentric distribution of colours (blue, purple, yellow) in halite and absence of "*thermally-metamorphosed blue selvages*" implied by Kopylova et al. (2013). Photo G shows a close-up of the nodule in the kimberlite boulder on Fig. 3D that was exposed to weathering in the stock pile for at least 3 years. Photo H shows the freshly exposed surface of the same nodule.

$_2SO_4$), arcanite (K_2SO_4) and thenardite (Na_2SO_4), are relatively minor, but widespread in halite fringing the outermost rims of carbonate sheets (Fig. 3 in Kamenetsky et al., 2007a); they are also present as inclusions in shortite and apatite (Fig. 7C–F). Shortite $Na_2Ca_2(CO_3)_3$ was found in close association with Cl-bearing Na–Mg carbonate northupite ($Na_3Mg(CO_3)_2Cl$). Well-formed and clear crystals of shortite (subsolidus modification of liquidus Na-Ca carbonates) and northupite

were used for studying melt and mineral inclusions (Kamenetsky et al., 2007a). Halite and shortite include euhedral crystals of zoned apatite and phlogopite, as well as tetraferriphlogopite, Ba-rich phlogopite, northupite, djerfisherite, rasvumite, K–Na and Na–Ca carbonates and sulphates, Ba-, Ca- and Sr-Ca-Ba-sulphates and carbonates, calcite, olivine, perovskite, bradleyite ($Na_3Mg(PO_4)(CO_3)$) and Mg–Ti–Fe spinel (Fig. 7). Apatite contains numerous inclusions along growth planes; the

inclusions are composed of halite, sylvite, Na–K–Ca carbonates, aphthitalite, and thenardite (Fig. 7C–F).

2.5. Radiogenic isotopes

The radiogenic isotope data for the UE kimberlite groundmass ($^{87}Sr/^{86}Sr_t \approx 0.70336$–$0.70505$, $\varepsilon_{Nd} \approx +2.8 - +4.6$, $^{206}Pb/^{204}Pb_t \approx 18.7$, $^{207}Pb/^{204}Pb_t = 15.53$, $^{208}Pb/^{204}Pb_t = 38.5$–$38.9$, t = 367 Ma; Maas et al., 2005) fall within the field defined by most group-I kimberlites (Smith, 1983; Fraser et al., 1985; Weis and Demaiffe, 1985). The Sr–Nd–Pb isotopic ratios of the silicate and carbonate components in the groundmass of the Udachnaya-East kimberlite support a mantle origin, as do the Sr–Pb isotope ratios in groundmass halide. Small differences between silicates and carbonates/chlorides, most clearly seen in initial $^{87}Sr/^{86}Sr$, are attributed to the extreme instability of magmatic halides and alkali carbonates in air, even on the timescale of hours and days (Zaitsev and Keller, 2006), possibly leading to minor modification of Rb–Sr isotope systematics in these assemblages since kimberlite emplacement (Exley and Jones, 1983; Maas et al., 2005; Paton et al., 2007; Kamenetsky et al., 2009c; Woodhead et al., 2009).

Possibly the most reliable way to estimate the Sr isotopic composition of the original kimberlite magma is the study of groundmass perovskite intergrown with olivine, phlogopite, shortite and halide minerals (Fig. 8; Kamenetsky et al., 2009c). Perovskite (CaTiO$_3$, Sr >1000 ppm, Rb/Sr ≈ 0) records and preserves the $^{87}Sr/^{86}Sr$ of the kimberlite melt at the time of perovskite formation (Heaman, 1989; Paton et al., 2007). $^{87}Sr/^{86}Sr$ in 20 individual perovskite grains analysed by LA-MC-ICPMS averaged 0.70312 ± 5 (2se), similar to the results of solution-mode isotopic analysis of other grains from the same perovskite population (0.70305 ± 7; Kamenetsky et al., 2012b). These Sr isotope ratios are lower than those for the acid-leached kimberlite groundmass (0.7034–0.7037, Maas et al., 2005). Such offsets between perovskite and host kimberlite were also noticed in other studies (e.g., Paton et al., 2007; Woodhead et al., 2009) and
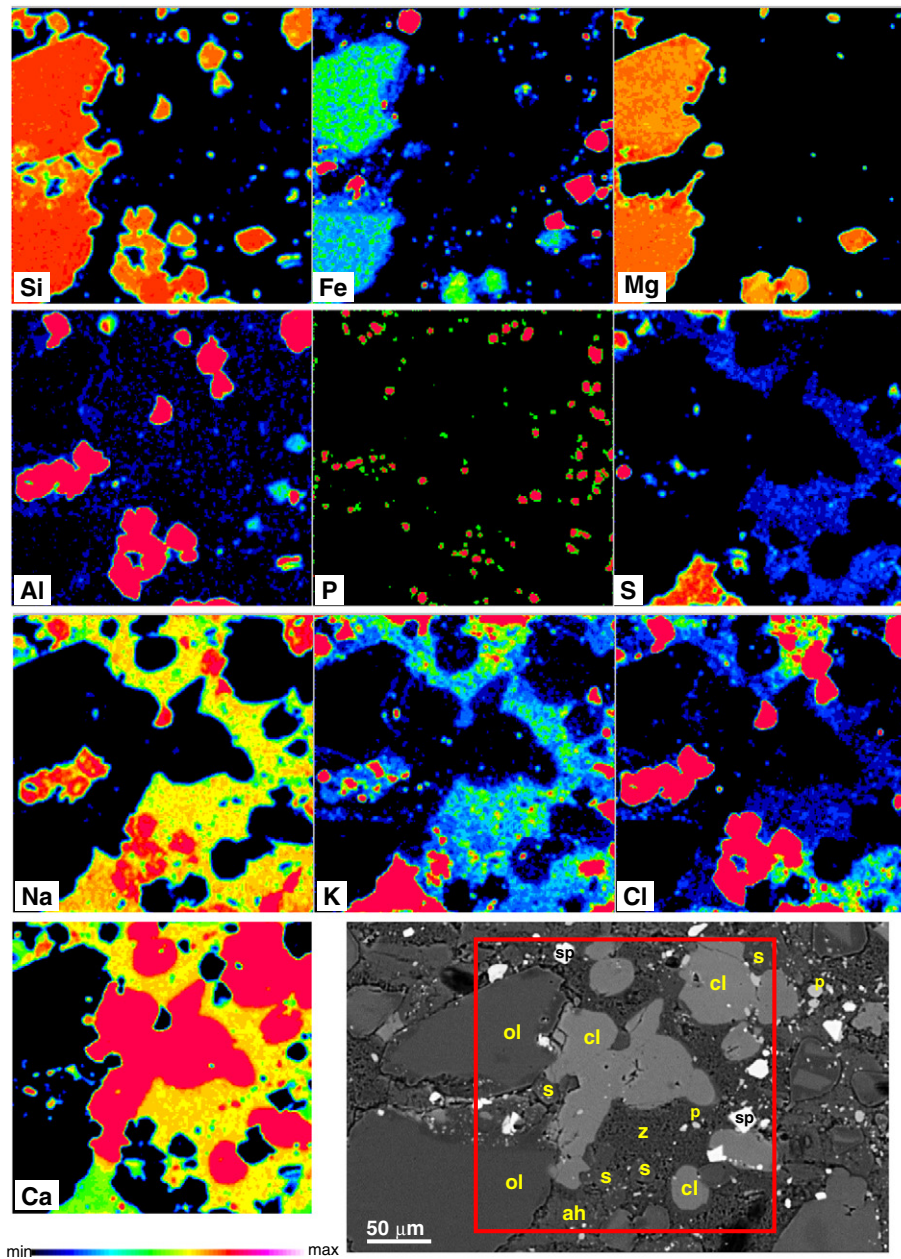

Fig. 5. Back-scattered electron image and X-ray element maps of the Udachnaya-East kimberlite (K-1), showing typical minerals: olivine (ol), calcite (cl), sodalite (s), nyerereite/zemkorite (z), aphthitalite (ah), Cr-spinel (sp), perovskite (p) and apatite (on the phosphorus map).
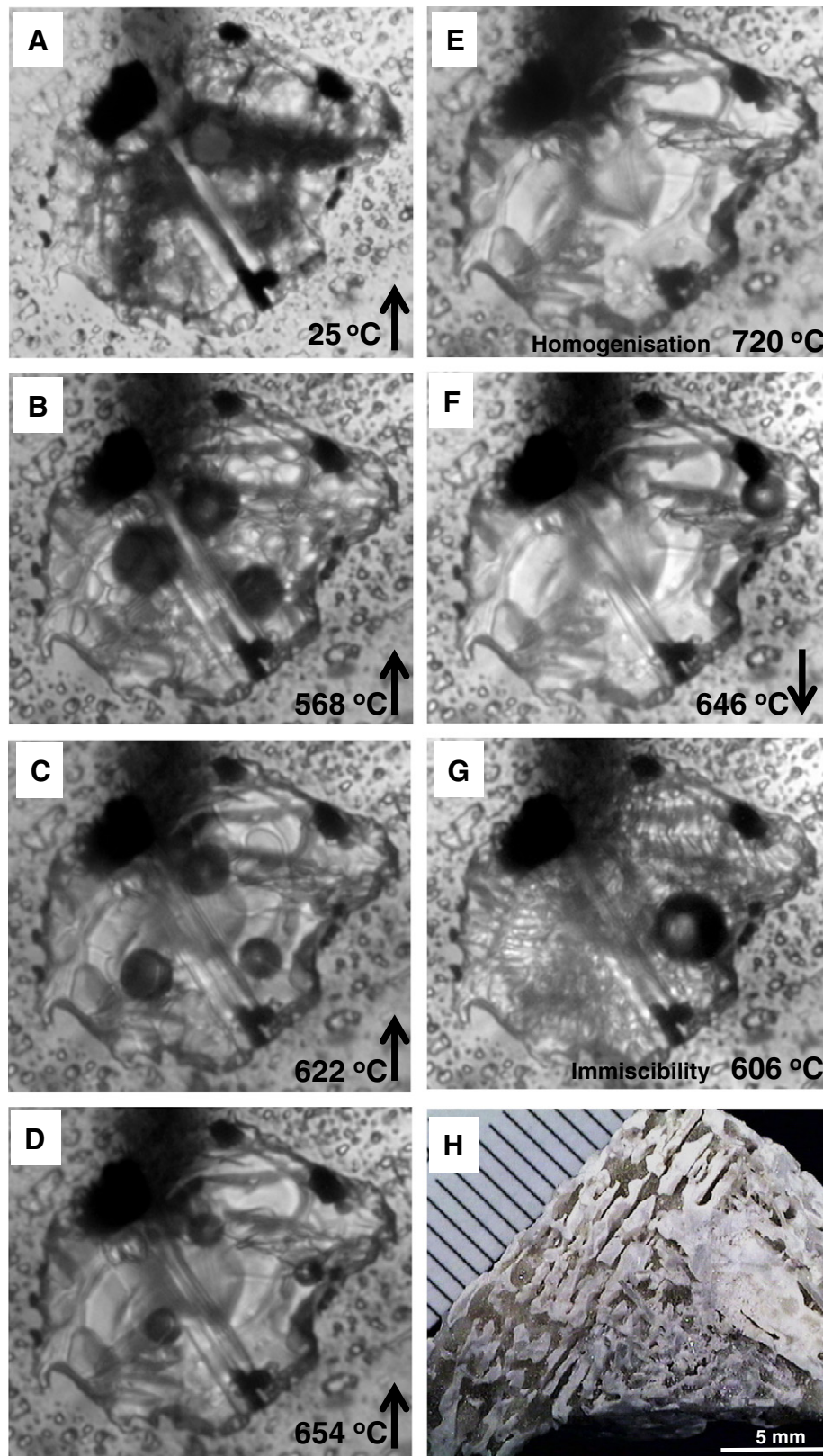
Fig. 6. Transmitted light photographs (A–G) showing phase transformations during experimental heating and cooling of an olivine-hosted melt inclusion (~55 μm) from the Udachnaya-East kimberlite. Complete homogenisation (melting of solid phases, miscibility of liquids and dissolution of vapour bubbles (dark spheres)) was achieved at 720 °C (E). During cooling, needle-like crystals and a bubble appeared at 646 °C (F), followed by instantaneous immiscibility between carbonate and chloride liquids at 606 °C (G). A fragment of the segregation in the groundmass, composed of skeletal alkali carbonate "sheets" in a fine-grained chloride matrix, shows texture resembling liquid immiscibility (H).

Fig. 7. Backscattered electron images showing mineral assemblage in carbonate-chloride nodules from the Udachnaya-East kimberlite (A, B). Main phases are represented by chlorides (halite and sylvite), shortite (sh), calcite (cl), phlogopite (ph), apatite (ap) and northupite (n). Euhedral apatite crystals contain 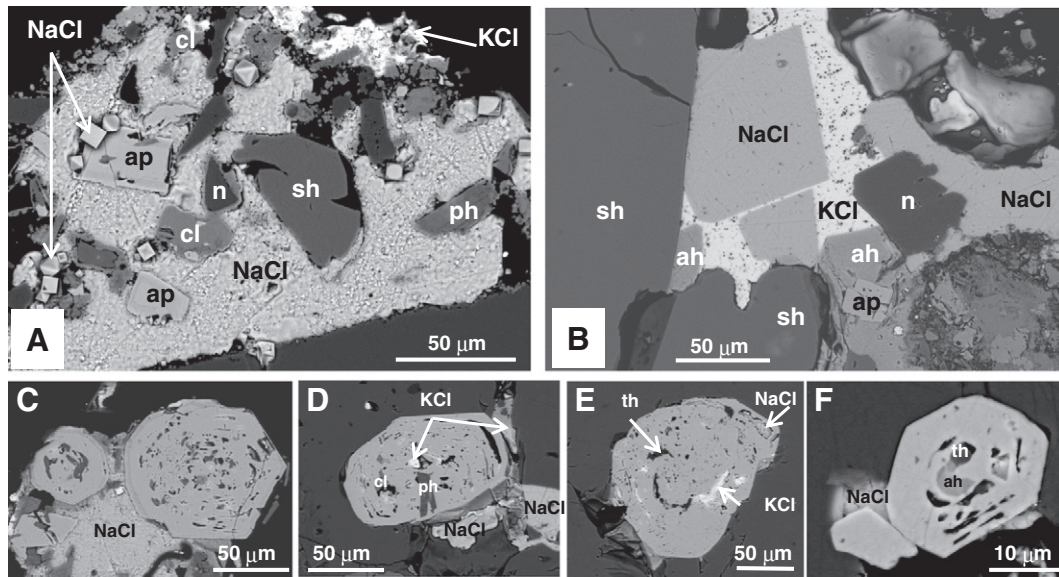abundant inclusions of chlorides, alkali sulphates — aphthitalite (ap) and thenardite (th), and phlogopite entrapped along concentric growth zones (C-F).

probably reflect minor disturbance of bulk rock Rb–Sr systems. The perovskite-derived Sr isotope ratios are therefore considered a more robust estimate of the kimberlite melt $^{87}Sr/^{86}Sr_i$. A ratio of ~0.7031 is among the most unradiogenic values recorded for archetypal kimberlites (Smith, 1983; Smith et al., 1985; Nowell et al., 2004), including those from Siberia (Kostrovitsky et al., 2007), and similar to ratios for modern oceanic basalts.

In an attempt to sidestep possible problems – alluded to above – with modification of carbonate and halide Rb–Sr isotope systematics during contact with air moisture, we performed step-leach experiments aimed at analysing $^{87}Sr/^{86}Sr$ in water-soluble minerals within melt inclusions in the UE olivine-II. Handpicked groundmass olivine grains from K-1 sample were carefully washed with distilled water and dilute nitric acid to remove soluble surficial material. The dried olivine grains were then ground to powder and sequentially leached with water and dilute acid, followed by dissolution of the residue with HF–HNO$_3$–HCl. Both leachates (water, UVK1L1; acid, UVK1L2) contain appreciable amounts of Rb and Sr (Table 1). After age-correction to 367 Ma, initial $^{87}Sr/^{86}Sr$ in these fractions is near 0.7042, within the range found for step-leached UE groundmass samples (Maas et al., 2005). The residue (UVK1R) has a surprisingly high Rb/Sr ratio ($^{87}Rb/^{86}Sr = 1.45$) and present-day $^{87}Sr/^{86}Sr$ (0.710422, Table 1), but the age-corrected $^{87}Sr/^{86}Sr$ is 0.70296, even slightly lower than the perovskite-based estimate of the magmatic $^{87}Sr/^{86}Sr$ (0.70305). Samarium and Nd would be expected to show much smaller solubility contrasts, and calculated initial ε_{Nd} values in UVK1R and UVK1L2 (the water leach did not have sufficient Nd for isotopic analysis) are indeed indistinguishable ($+4.3, +3.9$, Table 1) as expected if the silicate-oxide fraction of the kimberlite and olivine-hosted melt inclusions are comagmatic.

2.6. Stable isotopes

The carbonate component of the Udachnaya-East kimberlite has $\delta^{18}O$ values in the range of $+12$ to $+21‰$, and corresponding $\delta^{13}C_{PDB}$ values between $-1.6‰$ and $-5.3‰$ (Kamenetsky et al., 2012b). These $\delta^{13}C$ values, and their average ($\delta^{13}C = -3.38‰$) are within the range reported for other Siberian kimberlites (Kharkiv et al., 1991), and identical to the average $\delta^{13}C$ in kimberlites from the northern Yakutian fields

(Kopylova et al., 2013). The isotopic range of the carbonate-chloride nodules ($\delta^{18}O = 12.5$ to $13.9‰$; $\delta^{13}C = -3.7$ to $-2.7‰$; Kamenetsky et al., 2007a) is similar to that of the groundmass carbonates. These carbonate C–O isotope ranges are largely distinct from those in local limestones ($\delta^{18}O = 23$ to $26‰$; $\delta^{13}C = -2$ to $+2‰$; Kharkiv et al., 1991) and modern brines ($\delta^{18}O = -16.5$ to $-1.9‰$; Alexeev et al., 2007).

Although the carbon isotope composition of the studied UE carbonates is within the compositional range defined for mantle diamonds (-8 to $-2‰$; Cartigny, 2005; Giuliani et al., 2014) and the majority of kimberlites worldwide (e.g., Deines and Gold, 1973; Kobelski et al., 1979; Deines, 1989; Kirkley et al., 1989; Price et al., 2000; Fedortchouk and Canil, 2004; Giuliani et al., 2014), it is outside the "*probable field of primary igneous carbonatites*" ($\delta^{13}C -8$ to $-5‰$; as originally defined by Taylor et al., 1967). Variations in carbonatite $\delta^{18}O$ values (up to $+26‰$) have been ascribed to "*low-temperature deuteric or hydrothermal recrystallization of primary intrusive carbonatite*" (Taylor et al., 1967). This is confirmed by studies of modern natrocarbonatite lavas at Oldoinyo Lengai, Tanzania, where $\delta^{18}O$ magmatic values of $+6.5‰$ increased to $+11.8 - +12.4‰$ within days of eruption, concomitant with partial replacement of magmatic carbonates by hydrous Na–Ca carbonate–gaylussite (Keller and Hoefs, 1995; Keller and Zaitsev, 2006; Zaitsev et al., 2008). As equilibration with atmospheric moisture progresses, $\delta^{18}O$ increased even more, reaching $+15.5 - +18‰$ in the pirssonite carbonatites and $+23 - +27‰$ in the calcite carbonatites. Similarly, altered natrocarbonatite lavas from the ancient Tinderet and Kerimasi volcanoes are characterised by heavier $\delta^{18}O$ composition ($+16.2 - +22.6‰$) compared to primary calcite phenocrysts ($+7.4 - +8.1‰$; Zaitsev et al., 2013).

By analogy, carbonate stable isotope compositions in UE kimberlite samples from mine stockpiles might record similarly rapid isotopic exchange effects. Having noticed that primary magmatic Na–Ca carbonate minerals in UE kimberlite material exposed in polished sections and blocks (prepared in kerosene rather than water) show strong interaction with air moisture resulting in rapid (overnight) recrystallisation to H$_2$O-bearing carbonates (pirssonite, trona, hydrocalcite; Fig. 4 in Kamenetsky et al., 2012b), we tested this hypothesis with simple laboratory experiments. Carbonate samples with low $\delta^{18}O$ were
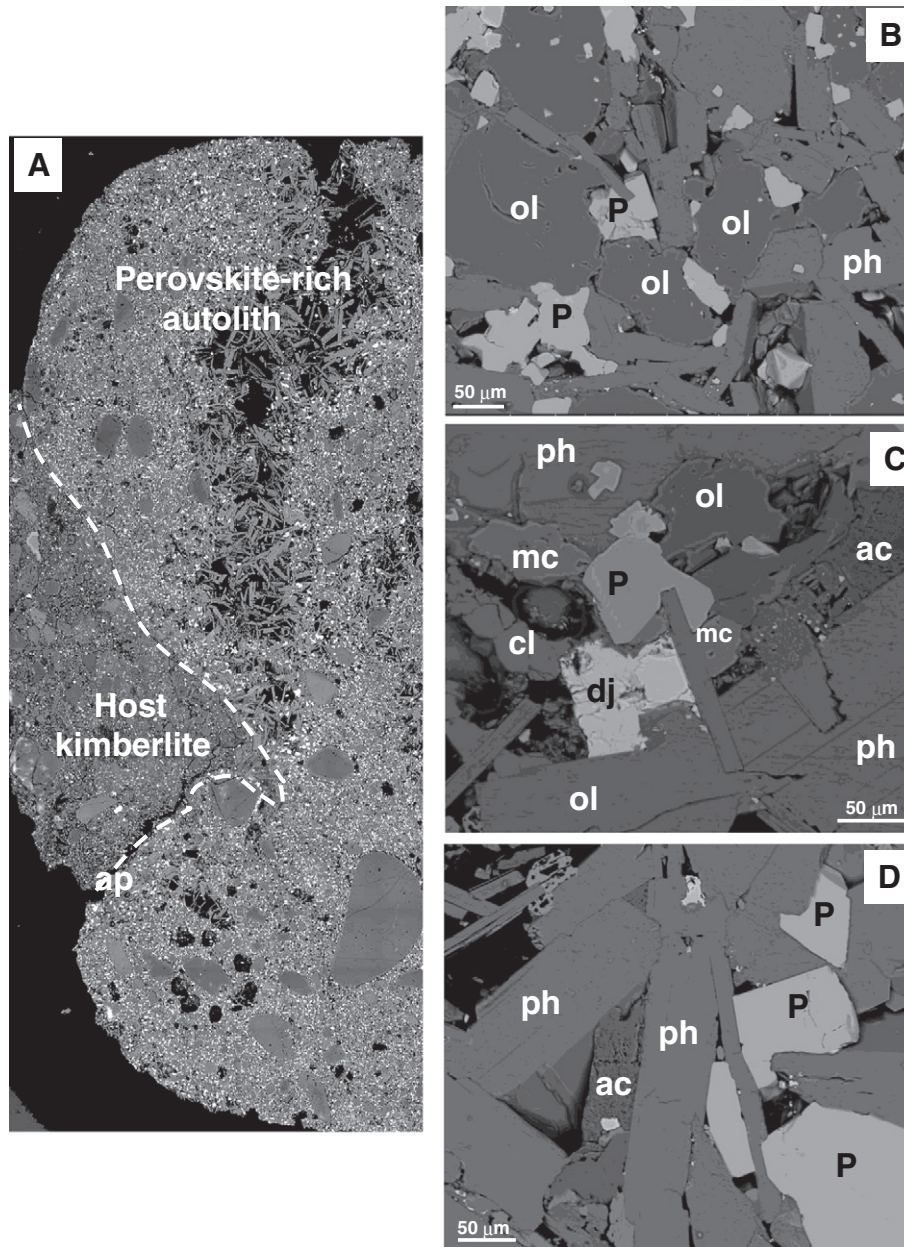
Fig. 8. Backscattered electron images showing contact of the perovskite–phlogopite–carbonate–olivine nodule and host Udachnaya-East kimberlite (A) and relationships between main minerals of the nodule (B–D): perovskite (p), alkali carbonates (ac), phlogopite (ph), djerfisherite (dj), olivine (ol), calcite (cl) and monticellite (mt). Note numerous cavities (black) that were formerly occupied by chloride minerals and interstitial occurrence of perovskite that justifies its late magmatic crystallisation.

subjected to wetting-drying cycles to test their sensitivity to rapid isotopic exchange. The resulting isotopic changes are minor for $\delta^{13}C$ (max increase 1.06‰, average 0.33‰), but significant for $\delta^{18}O$ (increase by up to 6.4‰, average 3.5‰; Table 2).

Sulphur isotope compositions of three bulk rock K-1 samples have $\delta^{34}S$ values of 1.0–2.2‰ for the sulphide (monosulphide + disulphide) and 14.3–14.5‰ for the sulphate components (Giuliani et al., 2014). In contrast, a K-2 sample is characterised by higher $\delta^{34}S$ values for sulphide and sulphate components (4.5 and 19.7‰, respectively).

3. The composition of Udachnaya-East kimberlite — implications for kimberlite melts

The association of fresh olivine (no serpentine minerals), phlogopite, apatite, sodalite, Cr-spinel and perovskite with alkali carbonates and chlorides in the groundmass of the UE kimberlite (type K-1), and the underlying chemical characteristics implied by this assemblage (high Na, Cl and CO_2, low H_2O), were used to propose a new composition for primary kimberlite melts (Kamenetsky et al., 2008). It was argued that kimberlite melts originate in the mantle as a chloride-carbonate liquid, devoid of "ultramafic" or "basaltic" aluminosilicate components. During ascent, such melts entrain xenocrystic material to which is partially dissolved or passively carried, resulting in an olivine-laden and olivine-saturated magma (Kamenetsky et al., 2008, 2009a,b, 2012b).

This radical departure from the orthodox view of kimberlite petrogenesis has been challenged vigorously, most recently in Kopylova et al. (2013) and Kostrovitsky et al. (2013). These authors assert that observations at Udachnaya-East do not require revision of existing kimberlite petrogenetic models because "salty" UE kimberlite can be explained by 1) heavy contamination of a common kimberlite magma by salt beds in sedimentary country rocks, or by 2) postmagmatic alteration by local groundwaters enriched in sodium chloride.

Table 1
Rb–Sr and Sm–Nd element and isotopic compositions of groundmass olivine-II, bearing melt inclusions, from the Udachnaya East K-1 kimberlite.

	UVK1L1	UVK1L2	UVK1R
Weight, mg	1.8	18	180
Rb ppm	42.6	8.24	1.28
Sr ppm	156.9	28.20	2.54
$^{87}Rb/^{86}Sr$	0.785	0.845	1.453
$^{87}Sr/^{86}Sr$	0.708233	0.708746	0.710422
Sm ppm		0.41	0.07
Nd ppm		2.74	0.56
$^{147}Sm/^{144}Nd$		0.0896	0.0773
$^{143}Nd/^{144}Nd$		0.512578	0.512573
ε_{Nd}		−1.17	−1.27
$^{87}Sr/^{86}Sr_i$	0.70420	0.70441	0.70296
ε_{Ndi}		+3.9	+4.3

Handpicked euhedral olivine grains (<1 mm in size, 0.5 g in total) were leached in distilled water (5 min) and 2 M nitric acid (2 min) in an ultrasonic bath, followed by additional exposure to cold 2 M nitric acid for another 10 min. After rinsing with water, the residual grains, assumed to be free of surficial chlorides and carbonates, were air-dried and powdered in a 10 ml agate ball mill. A split of the resulting powder (228 mg) was exposed to warm distilled water (80 °C, 30 min) and 2 M hydrochloric acid (80 °C, 30 min), to produce leachates UVK1L1, UVK1L2 and residue UVK1R, respectively. Mass loss during leaching amounted to 9.6%. UVK1R was dissolved in HF-HNO₃.
L1 = water leachate, L2 = dilute HCl leachate, R = residue. All analyses by isotope dilution. Elemental concentrations listed sample weights which rely on estimates of mass losses during leaching and carry considerable but unknown uncertainties. $^{87}Rb/^{86}Sr$ and $^{147}Sm/^{144}Nd$ have external precisions of ±0.5 and ±0.2%, respectively. Mass bias during MC-ICPMS analysis was corrected by normalising to $^{88}Sr/^{86}Sr$ = 8.37521 and $^{146}Nd/^{145}Nd$ = 2.0719425 (equivalent to $^{146}Nd/^{144}Nd$ = 0.7219), using the exponential law as part of an on-line iterative spike-stripping/internal normalisation procedure. Data are given relative to SRM987 = 0.710230 and La Jolla Nd = 0.511860. Internal precision (2se) is ±0.000020 (Sr) and ±0.000010 (Nd); external precision (reproducibility, 2sd) is ±0.000040 (Sr) and ±0.000020 (Nd). A split of the USGS basalt standard BCR-2 analysed in the same batch yielded 6.45 ppm Sm, 28.15 ppm Nd, $^{147}Sm/^{144}Nd$ 0.1384, $^{143}Nd/^{144}Nd$ 0.512628 (with 2 repeat runs: 0.512625, 0.512633) and $^{87}Sr/^{86}Sr$ of 0.705014 and 0.704951. One run of the JNd-1 Nd standard yielded 0.512111. All standard results are consistent with TIMS reference values. Initial ratios at 367 Ma. ε_{Nd} calculated for a modern CHUR composition of 0.1967 and 0.512638; depleted mantle model ages, T_{DM}, are given for a model depleted mantle with 0.2136 and 0.513151. The decay constants are: ^{87}Rb 1.395×10^{-11}/yr; ^{147}Sm 6.54×10^{-12}/yr.

3.1. Were kimberlite magmas contaminated by evaporite salts and brines?

A key point of the salt assimilation model by Kopylova et al. (2013) is that the Udachnaya kimberlite intruded through Middle Cambrian inter-reef lagoon sediments and Middle-Upper Cambrian cavernous dolomites with halite and gypsum cement. Such Cambrian salt-bearing sediments occur extensively in the southern part of the Siberian Platform (e.g., Fig. 1 in Alexeev et al., 2007). However, the northern boundary of the evaporite basin occurs at 64°N (Alexeev et al., 2007), some 220 km to the south of the Udachnaya pipe (66°25′N, 112°19′E). The stratigraphic basement-to-surface cross-section for the Udachnaya area (Fig. 2A) shows that neither evaporite salt deposits nor the so-called "lagoon sulfate-salt-carbonate rocks" (Fig. 7 in Kopylova et al., 2013) are present in the subsurface within at least 5 km of the

Table 2
Carbon and oxygen isotope compositions of the carbonate component in the Udachnaya-East kimberlites analysed by the same method in 2006 and 2013 years.

sample	2006 year		2013 year	
	$\delta^{13}C_{PDB}$	$\delta^{18}O_{SMOW}$	$\delta^{13}C_{PDB}$	$\delta^{18}O_{SMOW}$
K2-03	−4.795	12.345	−4.226	17.350
K24/04B	−3.596	12.773	−3.545	19.169
K4/05	−3.160	12.619	−3.154	13.923
K5/05	−3.223	14.384	−3.104	15.145
Uv-k1-05	−3.845	14.524	−2.784	18.469
Uv-k1-20a	−2.881	14.531	−2.561	18.356
K24/04	−3.443	12.964	−3.284	16.306

Details of the analytical method are presented in Kamenetsky et al. (2012b).

Udachnaya pipe. Furthermore, Alexeev et al. (2007, p. 227) contend that "Salt-bearing deposits and Na chloride brines typical of the Siberian Platform are lacking here. The groundwaters are saline waters and Ca or Mg chloride brines". Similarly, there is no record of salt beds in the logging reports for other drill holes in the vicinity of the Udachnaya pipe and the open mine pit down to 620 m.

The proponents of the assimilation model admit that "…the kimberlite does not intersect massive evaporites" (Kostrovitsky et al., 2013, p. 77), but suggest that the source of salts may be "…from the Upper Cambrian clastic dolomites of the Chukuck suite, or from the older and deeper Vendian or Lower Cambrian formations" (Kopylova et al., 2013). The porous-cavernous clastic/oolitic dolomites (not evaporites) of the Middle-Upper Cambrian Chukuckskaya suite in the area of the Udachnaya pipe are ~ 120 m thick and located below the present-day bottom of the mine pit (Fig. 2 and Fig. 8 in Alexeev et al., 2007). Claims of a lagoon-sabhka depositional environment and local concentrations of 20–30% halite for this sedimentary suite, attributed by Kopylova et al. (2013) to a report of Drozdov and Sukhov (2008), could not be confirmed. Instead, Drozdov and Sukhov (2008) noted that brines in these dolomites have a calcium-chloride composition.

In support of their alteration model for UE kimberlites, Kopylova et al. (2013) discuss several observations which they feel constitute evidence against a magmatic origin of high Na and Cl levels, alkali carbonate and chloride minerals in the groundmass, and chloride-carbonate nodules. Here we respond to some key points.

3.1.1. Carbonate-chloride "nodules"

Kopylova et al. (2013) ascribe the blue coloration of halite at the margins of salt "nodules" to thermal processing of sedimentary halite by "hot, 1000 °C, partially crystallized kimberlite magma". Our own observations indicate that the blue coloration has a patchy distribution (Fig. 4). Given the amount of sylvite in the halite (Fig. 3 in Kamenetsky et al., 2007a), the blue colour may therefore be caused by gamma-ray irradiation and associated structural damage related to ^{40}K decay (Howard and Kerr, 1960). Coloured patches in halite, observed in many rock salt occurrences, are not usually attributed to thermal metamorphism (e.g., Sonnenfeld, 1995).

We also reiterate that the carbonate-chloride "nodules" have textures reminiscent of liquid immiscibility at magmatic temperatures (Fig. 6 G, H), inconsistent with their origin as "evaporite xenoliths", as implied by Kopylova et al. (2013). Moreover, the mineral assemblage in the nodules (e.g., olivine, apatite, phlogopite/tetraferriphlogopite, perovskite, djerfisherite and rasvumite) is atypical of sedimentary rocks, and thus we are in position to infer magmatic origin for the alkali carbonate and chloride minerals. This is further supported by high-temperature melt inclusions in shortite, and abundant inclusions of halite, sylvite, Na–K–Ca carbonates, aphthitalite, thenardite and phlogopite/tetraferriphlogopite along growth planes in apatite (Fig. 7C–F) (see Kamenetsky et al., 2006, 2007a,b).

3.1.2. Radiogenic isotopes

Despite clearly comagmatic relationships between the perovskite and other groundmass minerals (olivine, phlogopite, shortite, calcite, sodalite, sulphide and halide minerals) in the UE kimberlite (Figs. 5, 8; Kamenetsky et al., 2009c), Kopylova et al. (2013) argued for "crustal contamination after crystallization of perovskite for the majority of the Udachnaya East and SFUE kimberlite". Kopylova et al. (2013) further claim that bulk UE kimberlite $^{87}Sr/^{86}Sr_i$ values are "outside of the global kimberlite values and a good match of the ratios with those of the Udachnaya brines, carbonate wallrocks and modern salt deposits". Our own published data show that $^{87}Sr/^{86}Sr$ ratios in modern brines at UE are much higher than in the UE K-1 groundmass and that sequential leaching of water-soluble (halite) and mild acid-soluble (carbonates) from halite-carbonate-rich K-1 groundmass extracts mantle-like radiogenic isotope signatures (Kamenetsky et al., 2004; Maas et al., 2005). We also note there is no obvious difference in Sr contents and Sr isotope
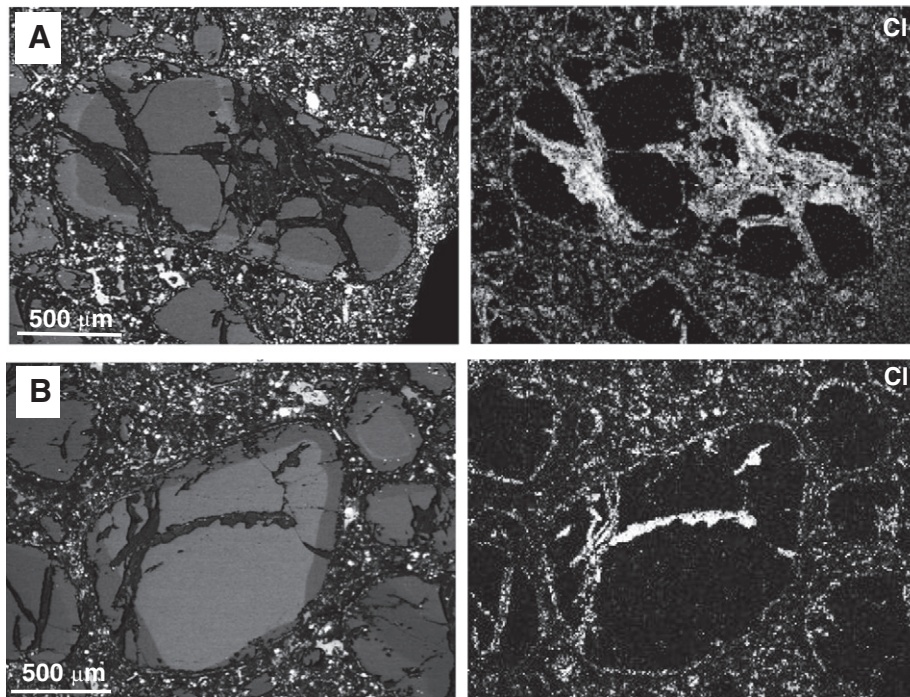
Fig. 9. Backscattered electron image and Cl Kα maps of the Jericho kimberlite, Canada (sample LGS-09, donated by M.G. Kopylova), showing presence of chlorine in serpentine replacing olivine along fractures and scattered in the groundmass.

ratios for kimberlites emplaced through evaporite-bearing sections of the Siberian kimberlite province and those for kimberlites from the northern fields, including Udachnaya ($^{87}Sr/^{86}Sr_i$ averages 0.7043 and 0.7041, respectively; Kostrovitsky et al., 2007).

Our experiments on 'sealed' salt-bearing melt inclusions within olivine phenocrysts reported above (see also Table 1) are of relevance here. These melt inclusions contain alkali carbonates and chlorides similar in composition to those in the K-1 groundmass. We assume that 'armoured' melt inclusions in olivine may not have experienced the late-stage (post-perovskite) contamination by crustal salty fluids inferred to have affected the K-1 groundmass (Kopylova et al., 2013). The unradiogenic, mantle-like $^{87}Sr/^{86}Sr$ compositions of these melt inclusions, and their similarity to equivalent results for the 'un-armoured' chloride-carbonate assemblage in the K-1 groundmass (Maas et al., 2005), indicate a lack of radiogenic isotope evidence for crustal assimilation in these samples, regardless of when such assimilation may have occurred.

3.1.3. Stable isotopes

Most Siberian kimberlites, including the studied UE, have high carbonate $\delta^{18}O$ values that are outside the so-called "*mantle carbonate box*" ($\delta^{18}O = +6 - +8.5‰$). This observation was cited as evidence for crustal contamination of UE K-1 kimberlite (e.g., Kjarsgaard et al., 2009; Kopylova et al., 2013). Differences in carbonate $\delta^{18}O$ between intrusive carbonatites and kimberlites (and extrusive carbonatites) have been noted in all studies of kimberlite carbonates. For example, Deines (1989) stated that "*only 7% of the kimberlite analyses fall in range from 6 to 9‰, and there is a strong maximum at about 12‰; similar to the values shown by many extrusive carbonatites*".

Given that extrusive carbonatites, known for their extreme sensitivity to reaction with air moisture, show carbonate $\delta^{18}O$ values that are higher than 'mantle carbonate', heavy oxygen in kimberlitic carbonate may be the result of exchange with deuteric and meteoric fluids (e.g., Giuliani et al., 2014), recrystallisation in air (our experiments

and Plyusnin et al., 1980), or isotopic exchange during sample preparation, especially if carbonates are water-soluble (e.g., alkali-carbonates). Importantly, the majority of samples showing very high $\delta^{18}O_{carbonate}$ values (>18–19‰) are kimberlite breccias, i.e. rocks more affected by exchange with hydrous fluids. If $\delta^{18}O$ values measured in UE primary carbonate minerals are adjusted for the maximum isotopic shifts observed in our experiments ($+3 - +4‰$, see above), $\delta^{18}O$ shift to values consistent with "mantle carbonate".

Kopylova et al. (2013) suggested that slightly negative $\delta^{13}C_{PDB}$ values in UE carbonates reflect contributions from crustal brines containing significant organic carbon ($\delta^{13}C = -10$ to $-12‰$). However, the stable isotope composition of modern brines in the Udachnaya pipe ($\delta^{13}C_{PDB} -16.8 - +1.7‰$; Alexeev et al., 2007) are inconsistent with the observed compositions of the UE carbonates.

In a crustal contamination scenario, local sources of heavy sulphur (5–44‰ $\delta^{34}S$, Vinogradov and Ilupin, 1972) would be expected to produce high $\delta^{34}S$ values in UE K-1, yet sulphides from the serpentine-free K-1 samples have low $\delta^{34}S$ consistent with derivation of S from a mantle source. Although the high $\delta^{34}S$ values of sulphates from serpentine-free samples of the UE kimberlite (14.3 to 14.5‰) might be suggestive of crustal contamination, $\Delta^{34}S_{sulphide-sulphate}$ values (12.2–13.5‰) for K-1 samples are consistent with sulphide-sulphate equilibration at ~500–550 °C (Giuliani et al., 2014). Such temperatures, and therefore high sulphate $\delta^{34}S$, are in turn consistent with microthermometric studies of melt inclusions hosted by olivine, shortite and phlogopite in the same samples (Kamenetsky et al., 2004; Golovin et al., 2007; Kamenetsky et al., 2007a, 2009c). We conclude that sulphur isotope results for UE K-1 support a mantle source of sulphur.

The chlorine isotope composition measured for halite from the carbonate-chloride nodule ($-0.18 - +0.3‰$ $\delta^{37}Cl$; Sharp et al., 2007) appears to be similar to values measured in mantle-derived rocks and chondrites (Sharp et al., 2007, 2013). Given that $^{37}Cl/^{35}Cl$ ratios in crustal rocks appear to be little different from those in mantle-derived rocks (and meteorites), using Cl isotope tracing to support an evaporite origin

of the UE chlorides (Kopylova et al., 2013) does not seem an appropriate means of obtaining conclusive evidence.

3.2. Did the "serpentine-free" kimberlite originate from interaction with groundwaters?

In their critique of a primary origin for alkali carbonate and chloride minerals in the groundmass of UE K-1 facies kimberlite, Kopylova et al. (2013) also discuss a possible secondary origin for the Na-Cl-S-bearing minerals through interaction with brines. One of the main arguments against such a process is that it cannot explain why olivine is not serpentinised. Instead, Kostrovitsky et al. (2013) proposed a kimberlite melt with unusually low H_2O content, as has been advocated in all publications by Kamenetsky and colleagues. Sr isotope evidence also does not support a major role for brine activity in producing the chloride mineral assemblage. $^{87}Sr/^{86}Sr$ in water and dilute acid leachates of the K-1 groundmass (0.7069 and 0.7050, respectively, before age correction) is much less radiogenic than in Sr-rich present-day brines in the mine pit ($^{87}Sr/^{86}Sr = 0.70885–0.70897$, Sr ~ 1000 ppm; Kamenetsky et al., 2004; Maas et al., 2005), and groundmass leachate radiogenic isotope ratios are mantle-like after age correction. This does not support the idea that modern brines or groundwaters may have affected K-1 isotopic signatures and mineralogy. A Late Palaeozoic Rb–Sr model age calculated for a salt segregation in the groundmass (Fig. 2 and Table 1 in Maas et al., 2005) rules out modern introduction of the salt (e.g., from the mine site brines). Moreover, initial Pb isotope ratios for this salt segregation and for other components in the K-1 groundmass are within the (overlapping) fields for group-1 kimberlite, MORB and OIB (we note that Pb isotope age corrections for this salt segregation are minimal, due to its extremely low $^{238}U/^{204}Pb$, see Table 1 and Fig. 3B in Maas et al., 2005).

Groundwaters in the two sedimentary aquifers hosting the Udachnaya kimberlite are highly concentrated Ca-chloride brines (up to 140 g/l in the upper aquifer and 320–380 g/l in the lower aquifer; Drozdov et al., 1989). The intersection of the lower aquifer with the UE kimberlite has a 200–250 m topographic "bulge", and its composition changes to dominantly Na-chloride (300 g/l, Drozdov et al., 1989). This dramatic local change in the groundwater composition (from Ca to Na-rich) was considered by Kopylova et al. (2013) to reflect Na introduction to groundwaters from country rocks, in marked contrast to the original hydrogeological interpretation that Na-rich groundwater was a result of interaction with Na-minerals in the kimberlite (Drozdov et al., 1989). If Na leaching from the kimberlite affects groundwater composition (Drozdov et al., 1989), the case for a kimberlite "replacement" model (Kopylova et al., 2013; Kostrovitsky et al., 2013) is seriously weakened.

4. Kimberlites worldwide: were they Na- and Cl-bearing prior to alteration?

4.1. Melt inclusions in olivine and Cr-spinel

We argued above that the UE parental kimberlite melt was enriched in alkali carbonate and chloride components, and this enrichment was inherited from the mantle source. We have further suggested that primary chemical characteristics of archetypal kimberlites are almost always affected, and even eradicated, by pervasive alteration. Good examples are the UE kimberlite breccia, the Udachnaya-West twin body and other kimberlites in the Siberian craton. This hypothesis was tested by studying melt inclusions entrapped in olivine, Cr-spinel and apatite in kimberlites (Kamenetsky et al., 2009b; Mernagh et al., 2011; Kamenetsky et al., 2013) emplaced into terranes composed predominantly of magmatic and metamorphic rocks (e.g., granite, diabase, gneiss, schist, quartzite, andesite). The studied samples include kimberlites from the Slave craton in Canada (Leslie, Aaron and Koala pipes in the Lac de Gras field, Jericho and Gahcho Kueʹ pipes), the North Atlantic

craton in southern Greenland (Majuagaa dyke) and the Kaapvaal craton in South Africa (Wesselton pipe).

Olivine grains hosting melt inclusions in the studied kimberlites from the Slave, North Atlantic and Kaapvaal cratons are indistinguishable from the UE kimberlite olivine (Kamenetsky et al., 2008) and belong to two populations (anhedral macrocrysts and euhedral zoned groundmass olivine) recognised in the archetypal kimberlites (Shee, 1985; Fedortchouk and Canil, 2004; Brett et al., 2009; Kamenetsky et al., 2009b; Arndt et al., 2010; Pilbeam et al., 2013). Crystallisation of groundmass olivine rims coincides with trapping of melt inclusions, which probably represent samples of parental melt. Multiphase melt inclusions occur in healed fractures in both olivine populations (thus secondary in origin) and are trapped in the groundmass olivine rims together with inclusions of phlogopite, Cr-spinel, perovskite and rutile. The melt inclusions are unlike those trapped in phenocrysts in other ultramafic and basaltic rocks, as they contain no silicate glass and aluminosilicate daughter minerals, except for minor phlogopite. Like UE K-1 facies melt inclusions, melt inclusions in olivine and Cr-spinel from other kimberlites worldwide contain crystal assemblages of calcite, dolomite, gregoryite (Na_2,K_2,Ca)CO_3, shortite $Na_2Ca_2(CO_3)_3$, nyerereite $Na_2Ca(CO_3)_2$, fairchildite ($K_2Ca(CO_3)_2$, eitelite $Na_2Mg(CO_3)_2$, burbankite ($Na,Ca)_3(Sr,REE,Ba)_3(CO_3)_5$, nahcolite $NaHCO_3$, pirssonite $Na_2Ca(CO_3)_2 \cdot 2H_2O$, hydromagnesite $Mg_5(CO_3)_4(OH)_2 \cdot 4H_2O$, bradleyite $Na_3Mg(PO_4)(CO_3)$, aphthitalite ($Na_{0.25},K_{0.75})_2SO_4$, northupite $Na_3Mg(CO_3)_2Cl$, aragonite, bassanite $CaSO_4 \cdot 5H_2O$, celestite, phlogopite, tetraferriphlogopite, magnetite, apatite, djerfisherite $K_6Na(Fe,Ni,Cu)_{24}S_{26}Cl$, halite and sylvite (Kamenetsky et al., 2009b; Mernagh et al., 2011; Kamenetsky et al., 2013). The bulk composition of the trapped melt cannot be reliably reconstructed from the inclusion data, because of reaction between the melt and the host minerals in the channel pathways, and the inevitable loss of water-soluble and unstable daughter minerals during sample preparation and analysis.

The alkali- and volatile-rich compositions of these melt inclusions are responsible for low-temperature phase transformations during heating experiments (Kamenetsky et al., 2009b, 2013). Melting occurs at <600 °C while carbonate-chloride liquid immiscibility and homogenisation occur at ~650–800 °C, well below the solidus of high-Mg melts traditionally thought to produce kimberlites. Notably, records of heating stage experiments with melt inclusions from different kimberlites are broadly similar.

4.2. Other indirect evidence: Na- and Cl-bearing minerals

Although melt inclusions provide direct information on melt compositions and temperatures, pervasive alteration of olivine in most kimberlites and unavailability of relevant research techniques to most investigators have severely limited the number of published melt inclusion studies in kimberlites to date. However, there exists a wealth of mineralogical and textural information that complement the melt inclusion evidence of Na- and Cl-bearing carbonate-rich compositions of archetypal kimberlite magmas.

Although Na-bearing kimberlites are sometimes reported (1–4 wt.% Na_2O; Siberia (Kostrovitsky et al., 2007; Vasilenko et al., 2002), NW Russia (Beard et al., 2000), India (Rao et al., 2004), Canada (Fedortchouk and Canil, 2004; Nowicki et al., 2008), South Africa (le Roex et al., 2003; White et al., 2012), Kenya (Ito, 1986), Colorado, USA (Meyer, 1976)), most kimberlites are exceptionally poor in Na_2O (<0.1 wt.%). The alleged "*sodium-poor environment*" of kimberlite melts has long been considered unfavourable to the formation of sodic minerals (Mitchell, 1986), and this view was echoed by others (e.g., "*unusual to find Na-rich minerals in kimberlite*" Scott Smith et al., 1983). This may go some way to explaining the scarcity of information on Na-bearing kimberlite groundmass phases. Rare occurrences of Na-bearing minerals in some kimberlites, such as pectolite $NaCa_2Si_3O_8(OH)$ (Agee et al., 1982; Kruger, 1982; Scott Smith et al., 1983; Ito, 1986;
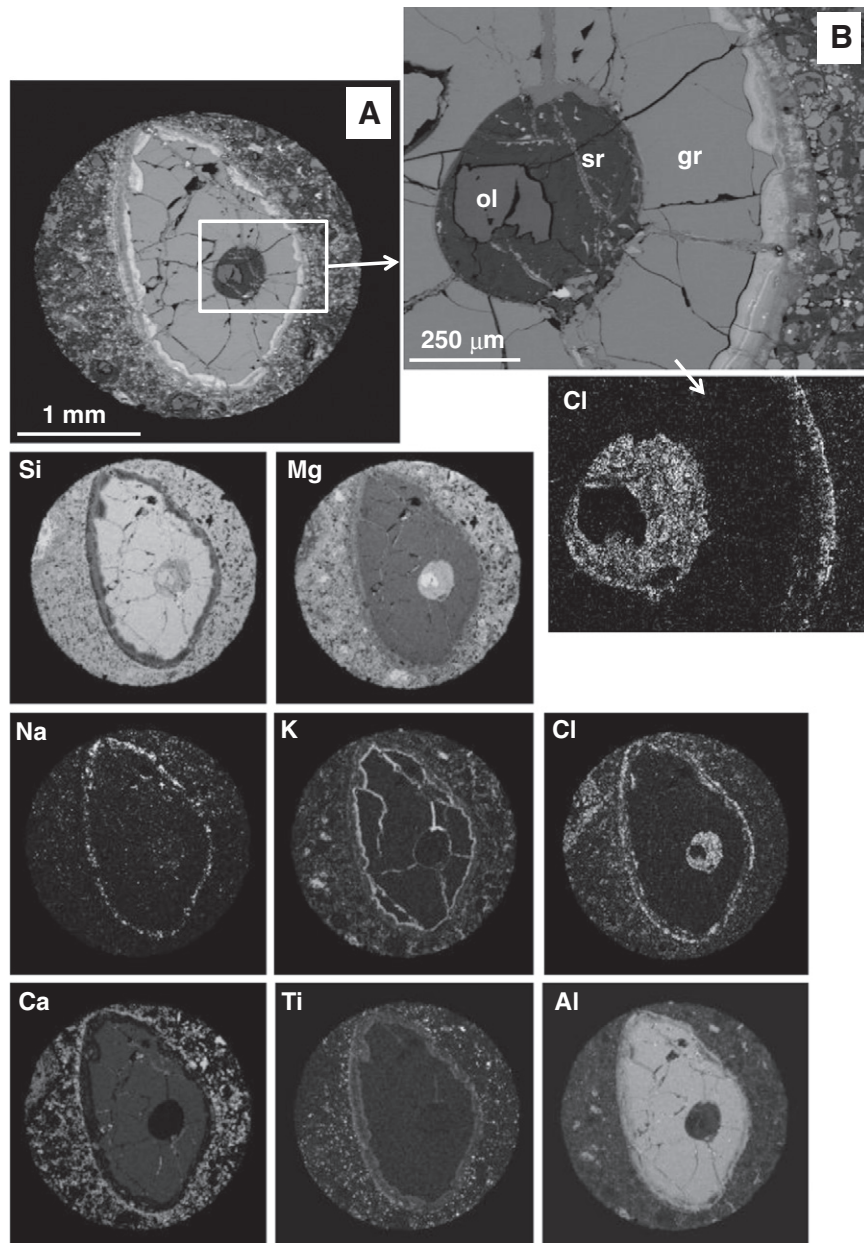
Fig. 10. Backscattered electron images and X-ray element maps of garnet macrocryst in the Jericho kimberlite, Canada (sample LGS-09, donated by M.G. Kopylova). Resorbed garnet (gr) contains olivine inclusion (ol), which largely replaced by Cl-bearing serpentine (sr). Alteration products of garnet (i.e., kelyphitic rim) are characterised by enrichment in Cl, Na, Ca and K.

Kopylova and Hayman, 2008), natrolite $Na_2(Al_2Si_3O_{10}) \cdot 2H_2O$, thomsonite $NaCa_2Al_5Si_5O_{20} \cdot 6H_2O$, cancrinite $Na_6Ca_2Al_6Si_6O_{24}(CO_3)_2$ (Ito, 1986), and chlorite-smectite (0.85–3.2 wt.% Na_2O; Mitchell et al., 2009) were interpreted as reflecting Na gain by the kimberlite melt upon assimilation of crustal rocks or introduction of crustal Na-bearing fluids (Scott Smith et al., 1983; Clement et al., 1984; Mitchell,
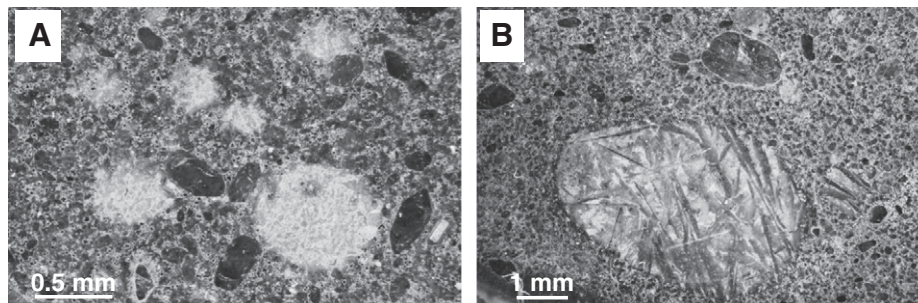

Fig. 11. Globular carbonate segregations with quenched texture in the carbonate-rich groundmass of the Diavik kimberlite, Canada (donated by R.C. Brett).

1986; Kopylova and Hayman, 2008). It is interesting to note in this context that sodic metasomatism of country rocks adjacent to kimberlites, chemically and mineralogically similar to fenitisation around carbonatite complexes, has often been recognised (e.g., Smith et al., 2004). We believe there is now sufficient reason to no longer dismiss Na-rich minerals in kimberlites, such as shortite (Watkinson and Chao, 1973; Cooper and Gittins, 1974), zemkorite (Egorov et al., 1988; Parthasarathy et al., 2002), Na-bearing calcite (Kamenetsky et al., 2013) and sodalite (Ito, 1986), as well as Na-Ba-bearing priderite ($K_2(Fe,Mg)_2Ti_6O_{16}$ (Chakhmouradian and Mitchell, 2001), Na-bearing phlogopite (up to 3 wt.% Na_2O; e.g., Emeleus and Andrews, 1975; Ito, 1986; Mitchell, 1978) and Na-bearing perovskite (up to 3 wt.% Na_2O; e.g., Boctor and Boyd, 1982; Chakhmouradian and Mitchell, 2000, 2001; Chakhmouradian et al., 2013) as secondary in origin and include this mineralogical evidence in a reappraisal of kimberlite parental melt compositions.

Magmatic halide minerals such as those preserved in the UE K-1 facies groundmass have never been reported in other kimberlites. However, they have analogues in the Oldoinyo Lengai natrocarbonatite lavas (Mitchell, 2006; Mitchell and Kjarsgaard, 2008) and Saint Honoré intrusive carbonatite (R. Mitchell, pers. comm.). The possible presence of magmatic salts prior to alteration and water-assisted sample preparation is usually impossible to ascertain conclusively, thus other indicators of magmatic Cl, such as sodalite and djerfisherite $K_6Na(Fe,Ni,Cu)_{24}S_{26}Cl$ (e.g., Dobrovol'skaya et al., 1975; Distler et al., 1987; Spetsius et al., 1987; Clarke et al., 1994; Chakhmouradian and Mitchell, 2001; Sharygin et al., 2003, 2007, 2008; Sharygin and Golovin, 2011) should be taken into account. Studies of chlorine concentrations in the alteration products of olivine (Egorov et al., 1991; Kamenetsky et al., 2009b; Spiridonov et al., 2010) are also instrumental in understanding compositions of deuteric and postmagmatic fluids in kimberlite rocks. Several generations of serpentine minerals, representing different stages of replacement of olivine grains and the groundmass by common groundwaters, are characterised by highly variable Cl content (e.g., 0.14–2.56 wt.%, average 0.84 wt.% in the Jericho kimberlite and 0.10–1.76 wt.%, average 0.53 wt.% in the Gahcho Kué´ kimberlite; Kamenetsky et al., 2009b). The Cl abundances are highest in the early serpentine adjoining olivine relics and inside fractures in olivine (Fig. 9), and become lower in subsequent serpentine generations (Fig. 9 in Kamenetsky et al., 2009b). Appreciable chlorine levels were recorded in the alteration products (also containing Na, K and Ca) of orthopyroxene and garnet megacrysts, and partially serpentinised (2 wt.% Cl) olivine inclusion in garnet in the Jericho kimberlite (Fig. 10). The presence of elevated Cl abundances in the earliest serpentine, combined with relative Cl depletion in later serpentine generations, implies that the chlorine contents of parental fluids were at their peak at the beginning of replacement and then gradually
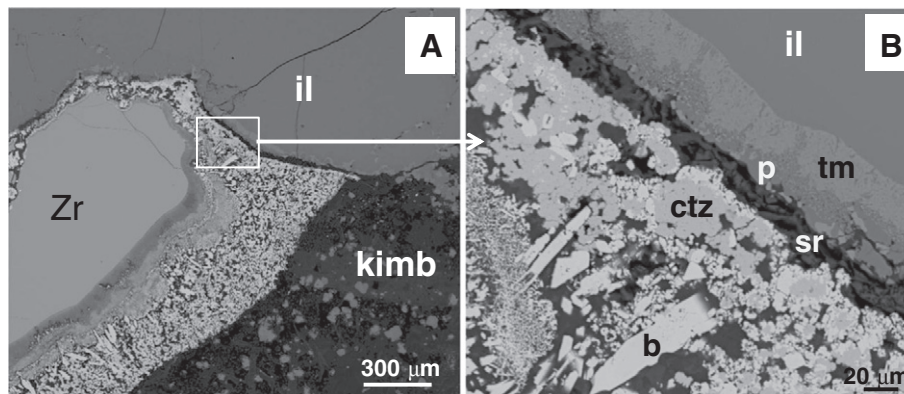

Fig. 13. Backscattered electron image and X-ray element maps of the exposed melt inclusion in ilmenite macrocryst from the Jericho kimberlite, Canada (sample LGS-09, donated by M.G. Kopylova), demonstrating presence of alkali-bearing carbonate, chloride, sulphate and phosphate daughter minerals.

decreased until complete exhaustion with further influx of meteoric waters. Such a scenario suggests that fluids that precipitated serpentine derived their chlorine budget either from residual kimberlite magmas and/or by dissolving magmatic salts in groundmass.

4.3. Other indirect evidence: carbonate–carbonate immiscibility

Textural studies of many kimberlites have demonstrated the occurrence of globular, amygdale-like and irregular pod-like segregations of intergrown calcite ± dolomite ± serpentine with minor phlogopite, apatite, monticellite and Fe–Ti–Cr oxides in a groundmass of similar composition (e.g., Dawson and Hawthorne, 1973; Clarke and Mitchell, 1975; Clement, 1975; Exley and Jones, 1983; Mitchell, 1984) reviewed

Fig. 12. Example of alteration mantles around zircon (zr) and ilmenite (il) megacrysts from the Monastery kimberlite (Kamenetsky et al., 2014) at the contact with host kimberlite (A) and each other (B). The mineral assemblages associated with 'alteration' of megacrysts in the kimberlite melt are represented by baddelyite (b), Ca–Ti–Zr oxides (ctz; calzirtite, zirkelite), perovskite (p), Ti–Fe oxides (tm), serpentine (sr), apatite, calcite, phlogopite, sphene, nepheline, kalsilite, K–Na titanites (priderite, freudenbergite) and Na–Zr silicates (catapleite).
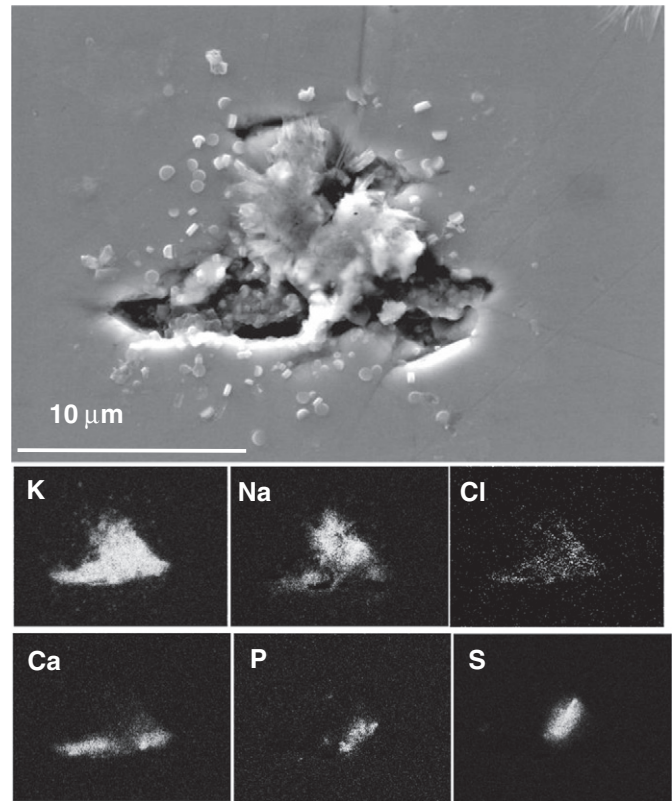
by Mitchell, 1986). The irregular shape of large carbonate segregations is probably a result of coalescence of neighbouring globules and wrapping of a carbonate liquid around olivine crystals (Fig. 4 B, C in Kamenetsky et al., 2013). Recent literature presents more examples of spectacular segregation textures in kimberlites (e.g., Diavik, Canada, Fig. 7A in Moss et al., 2009, Fig. 7B in Moss et al., 2008; Fig. 1E in Moss and Russell, 2011 and Fig. 11 (this work); Wesselton, South Africa, Fig. 8E in White et al., 2012; Ekati, Canada, Fig. 2 in Armstrong et al., 2004; Fig. 4 in Kamenetsky et al., 2013; Arkhangelsk, NW Russia Beard et al., 2000; Wekusko Lake, Canada, Fig. GS-5-3B in Chakhmouradian et al., 2006).

Most workers have argued for an undoubtedly magmatic origin of carbonate segregations in kimberlites (and carbonatites), based on their round and cylindrical shapes, quenched textures (Fig. 11), presence of other "hallmark" minerals of archetypal kimberlites, and enrichment of calcite in Na_2O, SrO and BaO (e.g., 0.37–0.65, 1.17–2.40, 2.37–4.18 in wt.%, respectively, in the Koala kimberlite, Canada, Kamenetsky et al., 2013). Carbonate segregations within matrix carbonate, although both principally calcitic in composition, provide a clue to significance of liquid immiscibility in the parental kimberlite melt (Clarke and Mitchell, 1975; Clement, 1975; Mitchell, 1984). Similar textures "*indicative of groundmass carbonate–carbonate immiscibility*", involving "*a Na–K–Ca–CO₂-rich, F-bearing fluid…and a Na-rich, Cl-poor carbonate liquid approximating to a nyerereite–gregoryite cotectic composition*" have been described for the natrocarbonatite lavas erupted from the Oldoinyo Lengai volcano (Tanzania) in 1995 (Mitchell, 1997). Thus, the immiscibility ("*emulsion-like*" after Clement, 1975) textures observed in many kimberlite may imply that liquids, compositionally different from calcite, were originally involved. Unusually Na-, Ba- and Sr-rich composition of calcite rhombs in the Ekati kimberlite segregations (Armstrong et al., 2004; Kamenetsky et al., 2013) suggest enrichment of former carbonatite liquids in alkali- and alkali-earth elements. Similar compositions of secondary calcite replacing nyerereite and shortite have been recorded in the Oldoinyo Lengai natrocarbonatite lavas, Tanzania (e.g., Keller and Zaitsev, 2006; Zaitsev and Keller, 2006; Zaitsev et al., 2008) and Tinderet calcified natrocarbonatite in Kenya (Deans and Roberts, 1984). If alkali carbonate rocks are prone to rapid degradation, as is the case for the Oldoinyo Lengai natrocarbonatites (Zaitsev and Keller, 2006), alkali carbonate parental liquids like those proposed for the UE kimberlite may be a significant component of parental magmas forming other kimberlites but are rarely preserved.

4.4. Constraints on Na₂O in kimberlite rocks and melts

Our understanding of primary sodium abundances in the kimberlite primary melt is intrinsically hampered by low Na_2O measured in most kimberlite rocks. The view that "*kimberlites that contain more than about 0.5 wt.% Na₂O are likely to have been contaminated. No primary mineral in kimberlite is a major host to sodium…*" (Clement et al., 1984) appears to be shared by many researchers. The alternative is that low Na in most kimberlites is a result of the near-ubiquitous alteration of kimberlites, and the degradation of alkali carbonate and chloride minerals and related mobility of sodium in hydrous fluids. Simple estimates suggest that Na, like other incompatible elements, should be high in low-degree partial melts generated from a mantle source. An estimate of expected Na abundances in kimberlite parental melts may be made using Na/Ti systematics. Na_2O/TiO_2 ratios are invariable during olivine crystallisation in primitive melts (i.e., in absence of plagioclase and magnetite) and liquid Na_2O concentrations in hypothetical parental kimberlite liquid might thus be estimated from (alteration-resistant) TiO_2 contents. The calculations below are made for mantle-derived silicate melts, i.e. we adopt the traditional model of an ultrabasic composition of kimberlite melts for the purposes of this exercise.

Primitive MORB (mid-ocean ridge basalt) liquids from the upper mantle show almost constant Na_2O/TiO_2 (2.21 ± 0.11 wt.%) over a range of melting conditions. Because kimberlite melts are inferred to originate at greater depths than MORB (e.g., presence of diamonds and "garnet signature"), the greater compatibility of Na at higher pressure (Putirka, 1999) implies that kimberlite melt Na_2O/TiO_2 would be lower than in MORB. Continental high-Ti olivine-saturated magmas are thus considered as a better analogy for kimberlites. High-Ti picrites from the Maimecha–Kotuy region in Siberia, Emeishan (SW China) and Karoo (South Africa) resemble kimberlites in having similar Ti-rich, Al-poor Cr-spinel compositions (Kamenetsky et al., 2001), enrichment in most incompatible elements, depletion in heavy rare-earth elements ("garnet signature") and comparable radiogenic isotope mantle signatures (Kogarko and Ryabchikov, 2000; Carlson et al., 2006). Homogenised olivine- and chromite-hosted melt inclusions from these rocks (e.g., Sobolev et al., 1992, 2009; Kamenetsky et al., 2012a) yield the lowest Na_2O/TiO_2 in terrestrial primitive melts (0.55 ± 0.05 in Siberian meimechites; 0.71 ± 0.11 in picrites from Emeishan and Karoo). If such Na/Ti ratios are applicable to UE kimberlites (0.85–1.87 wt.% TiO_2; average 1.25 ± 0.27 wt.% TiO_2; Kamenetsky et al., 2012b), Na_2O contents in the range 0.47–1.31 wt.% would be expected. Allowing for dilution with xenogenic olivine (25 to 50%; Mitchell, 2008; Brett et al., 2009), parental melt Na_2O could be 1.3–2 times higher. An independent estimate of 3–4 wt.% TiO_2 concentration in the kimberlite melt can be made using the composition of liquidus Cr-spinel in kimberlites (Kamenetsky et al., 2001). This yields Na_2O concentrations in the range 1.7–2.8 wt.%, broadly similar to estimates based on the average Na_2O content in kimberlitic perovskite (0.5 wt.%) and perovskite-silicate melt partitioning coefficients in the range 0.17–0.19 (Onuma et al., 1981; Chakhmouradian et al., 2013). Substantial Na_2O is thus expected even if kimberlites are derived from ultrabasic silicate melts. In our preferred natrocarbonatite-based model, high Na contents play a critical role (Kamenetsky et al., 2004, 2009b, 2012b, 2013).

5. Chemical fingerprint of alkali carbonate-chloride melts/fluids in mantle minerals

There is extensive evidence for the occurrence of alkali-rich carbonate melts and fluids in the Earth's mantle. The available evidence can be grouped in three categories: i) experiments performed under mantle P–T conditions; ii) carbonate metasomatism of mantle xenoliths sampled by kimberlite and alkali basalt magmas; and iii) direct observation of carbonate fluids/melts and their crystallisation products preserved as inclusions in mantle minerals, including diamonds.

A review of the extensive literature on experimental petrology that addresses mantle melting is beyond the scope of this paper. We briefly note that presence of alkali elements (± Cl) in starting materials bestows a strong enrichment in these elements to incipient carbonate melts and significantly reduces solidus temperature (e.g., Green and Wallace, 1988; Wallace and Green, 1988; Thibault et al., 1992; Dalton and Wood, 1993; Dasgupta et al., 2005; Safonov et al., 2007; Litasov and Ohtani, 2009; Safonov et al., 2011; Litasov et al., 2013).

5.1. Mantle xenoliths and megacrysts in kimberlites

Mantle xenoliths (both peridotites and eclogites) and individual megacrysts (pyroxene, olivine, garnet, ilmenite, zircon) often bear chemical signatures of carbonate metasomatism shortly before or during entrapment in kimberlite magmas (e.g., Konzett et al., 2000; Dawson et al., 2001; van Achterbergh et al., 2002; Misra et al., 2004; Giuliani et al., 2012, 2013b; Kamenetsky et al., 2014). The alkali-rich compositions of the inferred incipient and/or metasomatising melts are manifested by corresponding compositions of newly formed phases and melt inclusions in mantle minerals.

Eclogite xenoliths from the UE and other Siberian kimberlite demonstrate significant modifications of primary mineral assemblage, represented by the association of "spongy" clinopyroxene significantly depleted in Na and Al relative to original omphacite and complimentary

Na–Al-rich mineral (sodalite $Na_8Al_6Si_6O_{24}Cl_2$; Fig. 7 in Kamenetsky et al., 2009c) and multiphase "kelyphitic" rims around garnet (e.g., Solovjeva et al., 1997; Sobolev et al., 1999; Spetsius and Taylor, 2002; Misra et al., 2004; Shatsky et al., 2008; Spetsius and Taylor, 2008; Kamenetsky et al., 2009c). The secondary assemblage includes sodalite, calcite, shortite, dolomite, phlogopite-tetraferriphlogopite, halite, monticellite, djerfisherite, apatite, spinel, Ca–Ba–Sr sulphates, K-feldspar, Na-rich aegirine (10.9 wt.% Na_2O) and Cl-rich serpentine (0.55 to 2.15 wt.% Cl, Sobolev et al., 1999). Importantly, this secondary alkali-, chlorine and carbonate-bearing assemblage appears to host diamonds, whenever they are observed in-situ in eclogites (e.g., Anand et al., 2004; Spetsius and Taylor, 2008). Therefore, the chemical and mineralogical modifications of the eclogites were inferred to occur at mantle depths prior to or during formation of the kimberlite melt (e.g., Sobolev et al., 1999; Spetsius and Taylor, 2002; Misra et al., 2004). Similarly,

secondary sodalite and djerfisherite in peridotite xenoliths (e.g., Egorov et al., 2004; Sharygin et al., 2007; Pokhilenko et al., 2011; Sharygin et al., 2012) were considered important in characterising deep mantle fluids and melts and their relationships with kimberlites.

The relationships between alteration assemblages in mantle xenoliths and host kimberlite magma presents somewhat of a "the chicken or the egg" dilemma: alteration assemblages in mantle xenoliths could represent remnants of incipient kimberlite melt or they could be the product of reacting host kimberlite melt with mantle lithologies, or both (e.g., Bailey, 1980, 1984). A clear case of the kimberlite melt affecting mantle pyroxenes in the UE kimberlite (see Fig. 1 in Kamenetsky et al., 2009a) is represented by resorption, alteration and crystallisation of sodalite, djerfisherite and K-feldspar on pyroxene grain boundaries and along fractures. Essentially carbonatitic compositions of the melt/fluid reacting with mantle minerals are reflected in perovskite–Ti–Fe-
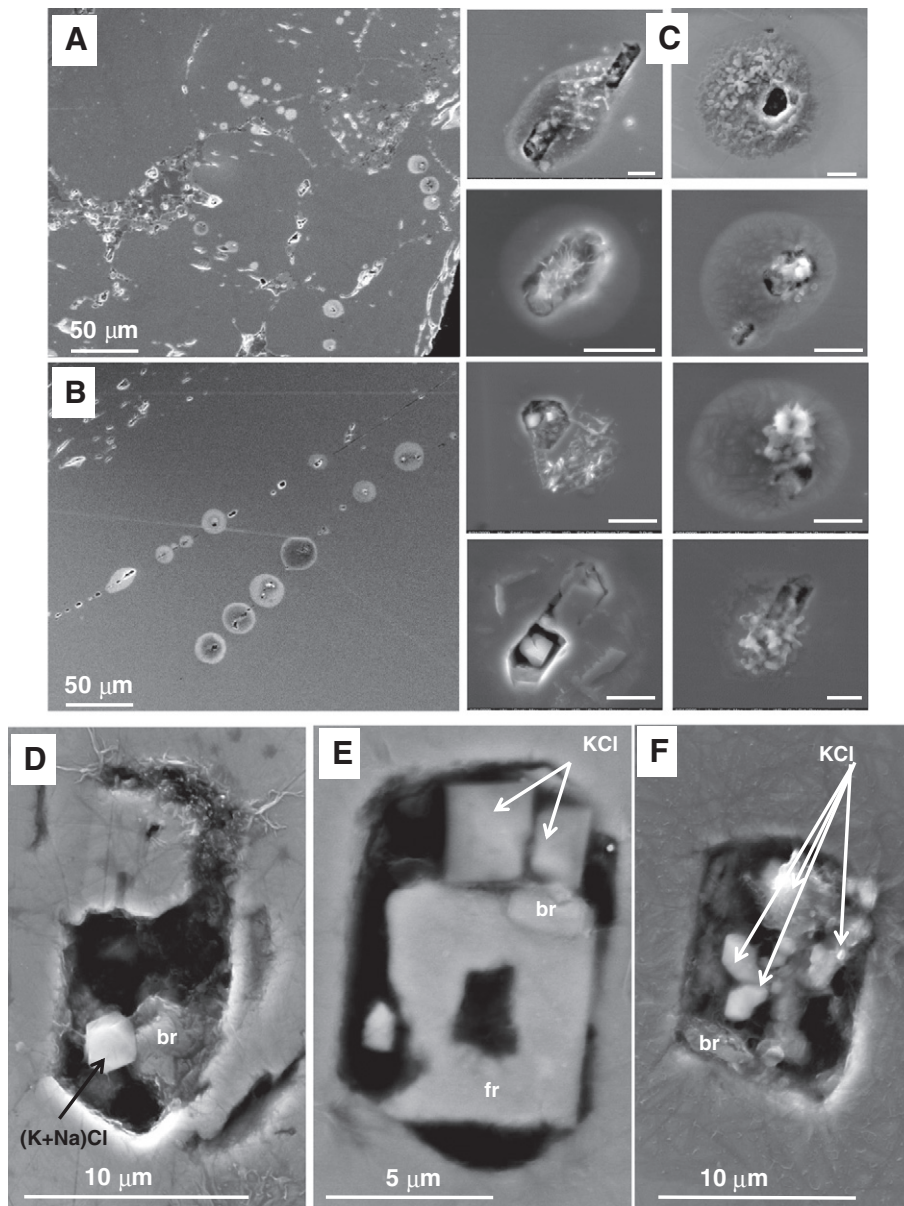

Fig. 14. Backscattered electron images of polished surface of ilmenite macrocrysts from the Wesselton kimberlite, South Africa (donated by R.H. Mitchell). Numerous melt inclusions occur in linear trails representing healed fractures in ilmenite (A, B). Melt inclusions intersected during polishing ooze water-soluble components that precipitate on the surface at equal distances (circle) from points of leakage (A–C). Most common daughter minerals in melt inclusions (C–F) are Na-K chlorides, alkali carbonates, bradleyite (br) — $Na_3Mg(PO_4)(CO_3)$ and freudenbergite (fr) — $Na_2Fe_2Ti_6O_{16}$. Scale on Fig. 14C is 5 μm.

oxide and baddelyite rims around picroilmenite and zircon megacrysts, respectively, in kimberlites worldwide (Fig. 12; see also Raber and Haggerty, 1979; Kamenetsky et al., 2014).

Crystallised melt inclusions dominated by carbonates (magnesite, dolomite, Ca–Na–K carbonates) with variable amounts of phosphates (apatite and bradleyite), kalsilite, phlogopite and minor olivine, spinel, sulphides, alkali-sulphates and chlorides were identified in ilmenite grains of mantle polymict breccia xenoliths from the Bultfontein kimberlite (Giuliani et al., 2012, 2013b). Nickel-rich mineralisation of mantle derivation in spinel harzburgite xenoliths from the same kimberlite are also characterised by compositionally similar inclusions (Ca–Na–K carbonates, phlogopite, Ca–Na–Mg phosphates, chlorides and sulphides) that are hosted by metasomatic olivine and spinel (Giuliani et al., 2013a). Abundant secondary melt inclusions, composed of water-soluble alkali-bearing carbonates, chlorides, sulphates and phosphates in ilmenite megacrysts (Figs. 13–15) from a number of well-known kimberlites (Udachnaya-East, Wesselton, Jericho, Majuagaa) support the common occurrence of alkali-carbonate melts in the mantle, at least in the mantle domains where megacrysts formed. Moreover, Cl-rich aqueous and carbonic fluid inclusions in basalt-hosted mantle xenoliths (e.g., Frezzotti et al., 2002, 2010) are considered pivotal in determining the composition of fluids in the lithospheric mantle.

5.2. Inclusions in diamonds

Kimberlite magmas are the most important carrier of diamonds and "… a number of studies have verified diamond nucleation and growth in a range of alkali- and chloride-rich C-bearing systems" (Shirey et al., 2013). The diamond-hosted inclusions are good indicators of fluids and melts present in the mantle source of kimberlites (Navon et al., 1988; Pal'yanov et al., 1999, 2002; Palyanov et al., 2007). Microinclusions in cubic fibrous diamonds, in fibrous coats of coated diamonds and in clouds within octahedral diamonds have been ascribed to four compositional end-members: high-Mg carbonatitic, low-Mg carbonatitic, silicic and saline high-density fluids (HDFs; Navon et al., 1988; Weiss et al., 2009 and references therein); all are enriched in alkali elements.

Saline compositions primarily enriched in Cl, K and Na (Fig. 16) were found in diamonds from the Koffiefontein, DeBeers-Pool and Koingnaas mines in South Africa (Izraeli et al., 2001; Weiss et al., 2008) and the Ekati (Panda) and Diavik mines and Wawa metaconglomerate in Canada (Tomlinson et al., 2006; Klein-BenDavid et al., 2007a; Smith et al., 2012). While the K_2O content of individual saline microinclusions varies mostly between 20–40 wt.% and is similar in different diamonds (Fig. 16A), the sodium content spans a larger range (<0.5–40 wt.% Na_2O, Fig. 16B) and differs between diamonds of different provenance (Fig. 16B). Saline HDFs in the Canadian diamonds have similar Na_2O levels: over 97% of microinclusions in the Diavik diamonds, 90% in the Wawa diamonds and 75% in the Panda diamonds vary between 4–18 wt.% Na_2O (excluding the more carbonatitic inclusions in Panda diamonds). HDFs in the DeBeers-Pool and Koingnaas diamonds have relatively higher levels of Na_2O with >66% containing >20 wt.% Na_2O (>97% containing >5 wt.% Na_2O). HDFs in the Koffiefontein diamonds have the lowest levels of Na_2O, <5 wt.% in over 85% of microinclusions. The average $(K + Na)/Cl$ molar ratio of saline HDFs is 1.1 ($\sigma = 0.3$), suggesting compensation of the alkalis by both Cl and carbonate ions. This is consistent with K- and Na-carbonate daughter phases in such inclusions (Klein-BenDavid et al., 2007b; Smith et al., 2011). Enrichment of alkalis is typical in silicic and carbonatitic HDFs as well. For example, silicic HDFs have typically 2–5 wt.% Na_2O and 10–20 wt.% K_2O (Schrauder and Navon, 1994; Shiryaev et al., 2005; Klein-BenDavid et al., 2009; Weiss et al., 2009; Zedgenizov et al., 2009), while the high-Mg carbonatitic HDFs, including those in the Udachnaya diamonds, have 7–14 wt.% Na_2O and 9–27 wt.% K_2O (Klein-BenDavid et al., 2009; Weiss et al., 2009). The high-Mg carbonatitic HDFs are closer in composition to kimberlites (Klein-BenDavid et al., 2009; Weiss et al., 2009, 2011); still these HDFs have higher alkalis even when compared to the exceptionally alkali-rich UE kimberlites.

Although there is no direct evidence that diamonds and kimberlites share the same parental fluid/melt, striking commonalities (similar Ca, K and Na) exist between saline HDFs in diamonds and melt inclusions trapped in olivine and ilmenite megacrysts from Udachnaya, Greenland and Wesselton kimberlites (Fig. 17). The megacryst-hosted melt inclusions (Fig. 14) vary in composition between low-Mg carbonatitic and Na-rich chloride melts. Most of the Udachnaya and Wesselton inclusions plot with the Na-rich HDFs in the DeBeers-Pool diamonds, whereas Greenland high-Ca inclusions are more similar to the low-Mg carbonatitic HDFs from Panda. These similarities together with generally elevated contents of alkalis in HDFs trapped in diamonds suggest
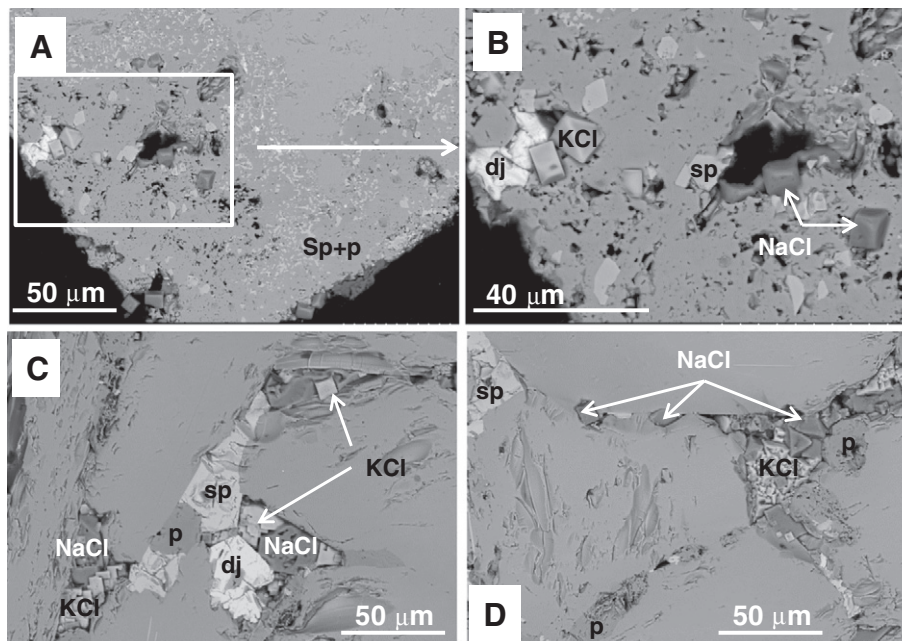

Fig. 15. Backscattered electron images of polished surface of ilmenite macrocrysts from the Udachnaya-East kimberlite, showing typical assemblage of perovskite (p), Fe–Ti spinel (sp), halite, sylvite, djerfisherite (dj) and Na–Ca carbonates in the alteration along the rims and fractures in ilmenite.
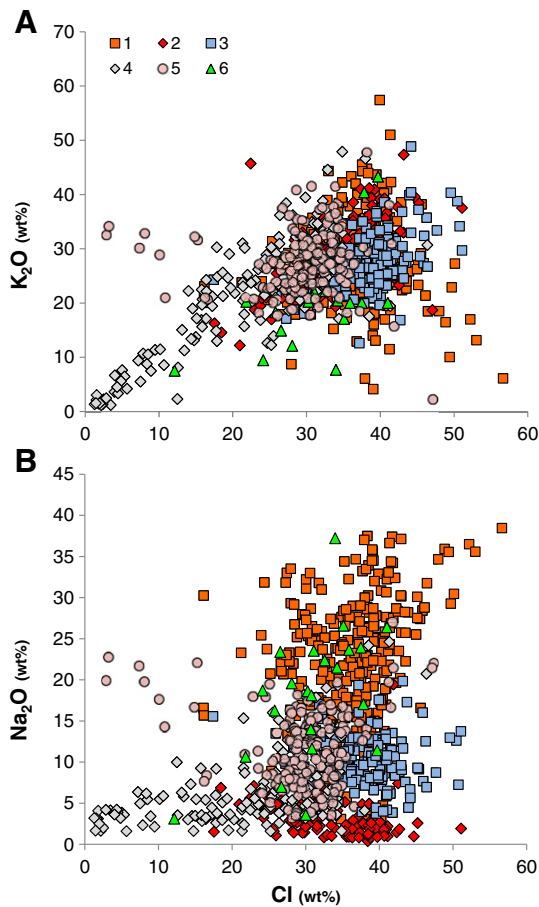
Fig. 16. Variation diagrams of (A) K_2O and (B) Na_2O against Cl in individual microinclusions of saline HDF compositions (all in wt.%, calculated on a water- and CO_2-free basis). Saline HDFs trapped in fibrous diamonds from South Africa and Canada have high levels of K_2O and Cl; some of the inclusions in the Panda diamonds are more carbonatitic in compositions, showing lower K_2O and Cl. The Na_2O contents vary significantly and differ between HDFs in diamonds from different origins; compared to the K_2O and Cl abundances showing a range that is similar in different diamonds. Data for inclusions in diamonds are from DeBeers-Pool (1), Koffiefontein (2), Diavik (3), Panda (4), Wawa (5) and Koingnaas (6), reported by Izraeli et al. (2001), Tomlinson et al. (2006), Klein-BenDavid et al. (2007a,b), Weiss et al. (2008), Weiss (2012) and Smith et al. (2012).

Fig. 17. Ternary diagram of $CaO–K_2O–Na_2O$ showing compositions of individual saline microinclusions in diamonds from DeBeers-Pool (1), Koffiefontein (2), Koingnaas (3), Panda (4), Wawa (5) and Diavik (6) and melt inclusions trapped in olivine (all generations) and ilmenite megacrysts from Greenland, Wesselton and Udachnaya-East kimberlites. The composition of Udachnaya-East and Wesselton melt inclusions fall among the Na-rich HDFs in DeBeers-Pool diamonds, while the melt inclusions from Greenland are more carbonatitic in compositions and resemble the more carbonatitic microinclusions from the Panda diamonds.

enrichment of K and Na in the mantle sources where kimberlite magmas are formed.

6. Towards a new petrogenetic model for kimberlites

Experimental studies of putative primary kimberlite compositions by Brooker et al. (2011) suggested that (i) bulk kimberlite rock compositions do not represent kimberlite melts because of accumulation of olivine, introduction of water and replacement of olivine and primary carbonates during post-magmatic alteration; (ii) previously inferred high liquidus temperatures (>1400 °C) are inconsistent with geological evidence (e.g., absence of thermometamorphic effects (Barrett, 1975; Clement, 1975; Edwards and Howkins, 1966; Mitchell, 1986) and palaeomagnetic data (Fontana et al., 2011)), temperatures in the potential mantle source, mineral paragenesis and thermodymanic modelling; and (iii) solubilities of H_2O and CO_2 in the model (ultramafic/ultrabasic) kimberlite melt at emplacement pressures are not as high as required by measured abundances of these volatiles in kimberlite rocks.

These conclusions support our hypothesis (Kamenetsky et al., 2004, 2008, 2009b,c, 2012b) that the parental (proto)kimberlite melt is virtually anhydrous, aluminosilicate-poor Na-Ca carbonate, which is enriched in lithophile trace elements, halogens, and sulphur. On arrival near the surface, these melts are relatively low-temperature (<800 °C)
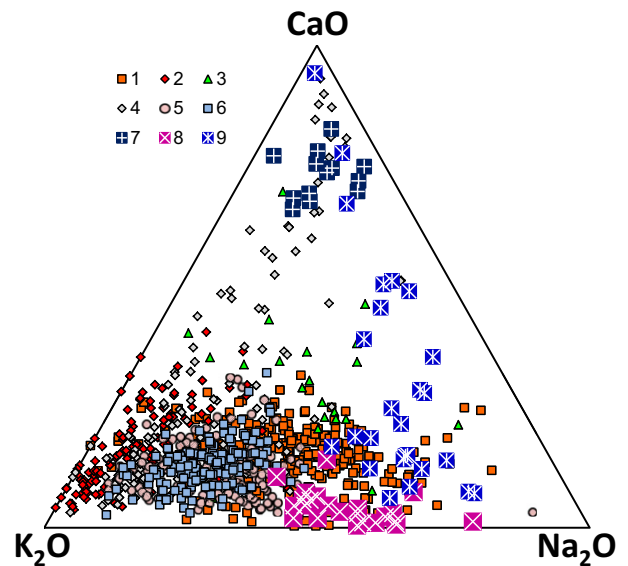
and have unique rheological properties that readily explain their fast ascent from mantle depths and their ability to carry heavy loads of mantle and crustal solids. The silica-undersaturated carbonatite liquid dissolves mantle silicates, especially orthopyroxene, on ascent. When the melt reaches olivine saturation at low pressure, olivine crystallisation occurs, which drives the residual melt towards the initial (protokimberlite) carbonatite composition.

Our model represents a major departure from the orthodox model which envisages kimberlite parent liquids as having ultrabasic/ultramafic, H_2O-rich and Na_2O-poor compositions (e.g., Kopylova et al., 2013). One of the main arguments against the new model has been the suggestion that the K-1 facies of the UE kimberlite is not the pristine, unaltered kimberlite we describe, but that its parent magma has been contaminated by crustal wallrocks and/or that the resulting kimberlite pipe, including the unique K-1 facies, was modified by saline groundwaters (Kopylova et al., 2013; Kostrovitsky et al., 2013). As part of this argument, the chloride-alkali carbonate groundmass assemblage and mineralogically similar "nodules", which are such conspicuous features in part of the UE pipe, are re-interpreted as manifestations of contamination by Cambrian evaporites. In other words, the same components we consider to be of mantle origin, related to the kimberlite parental melt and thus a key component of our new model, are interpreted by the proponents of a "classic kimberlite" as crustal contaminants.

In this paper we demonstrated that the serpentine-free sections of the UE kimberlite, on which all our observations are based, are not contaminated by evaporitic materials. Rather, this kimberlite owes its unusual petrochemical and mineralogical characteristics to a fortuitous lack of interaction with syn- and post-magmatic aqueous fluids, possibly because of "shielding" by the earlier magmatic phases (KB-3 and KB-4) and "conserving" effects of ductile chloride minerals in the groundmass (Kamenetsky et al., 2012b). The groundmass assemblage of this kimberlite, and earlier formed melt inclusions of similar composition, contain alkali carbonate, chloride and other Na- and Cl-bearing minerals which reflect enrichment of the parental melt in carbonate, chlorine and sodium. By contrast, other kimberlites from the Udachnaya pipe (both eastern and western bodies) and kimberlites worldwide

have mineral assemblages and bulk compositions that are depleted in Na and Cl, but enriched in H_2O.

The association of low H_2O and high Na and Cl abundances in the studied UE rocks with a lack of serpentine minerals, the dominant hydrous alteration style in the remainder of the Udachnaya pipes and in kimberlites elsewhere, and with remarkably alteration-free mantle xenoliths, provide compelling evidence for a magmatic, mantle-derived origin of these features. Compositional evidence for kimberlite liquids similar to those inferred at UE is recorded in melt inclusions in kimberlites from other cratons. These results strongly suggest that two key components of the orthodox kimberlitic magma model – low sodium and high water contents – are postmagmatic alteration features.

The results presented here clearly demonstrate that micro-analytical studies of kimberlites and other mantle-derived materials (macrocrysts, xenoliths, diamonds) provide powerful insights into kimberlite petrogenesis and related mantle processes. We invite collaborative projects that involve micro-analytical studies of individual mineral phases and melt inclusions in the least altered kimberlite samples from different localities.

Acknowledgements

References

Agashev, A.M., Ionov, D.A., Pokhilenko, N.P., Golovin, A.V., Cherepanova, Y., Sharygin, I.S., 2013. Metasomatism in lithospheric mantle roots: constraints from whole-rock and mineral chemical composition of deformed peridotite xenoliths from kimberlite pipe Udachnaya. Lithos 160, 201–215.

Agee, J.J., Garrison, J.R., Taylor, L.A., 1982. Petrogenesis of oxide minerals in kimberlite, Elliott county, Kentucky. Am. Mineral. 67, 28–42.

Alexeev, S.V., Alexeeva, L.P., Borisov, V.N., Shouakar-Stash, O., Frape, S.K., Chabaux, F., Kononov, A.M., 2007. Isotopic composition (H, O, Cl, Sr) of ground brines of the Siberian Platform. Russ. Geol. Geophys. 48, 225–236.

Alexseev, S.V., 2009. Cryogeological Systems of the Yakutian Diamondiferous Province. Academic Publishing House "GEO", Novosibirsk (319 pp.).

Anand, M., Taylor, L.A., Misra, K.C., Carlson, W.D., Sobolev, N.V., 2004. Nature of diamonds in Yakutian eclogites: views from eclogite tomography and mineral inclusions in diamonds. Lithos 77, 333–348.

Armstrong, J.P., Wilson, M., Barnett, R.L., Nowicki, T., Kjarsgaard, B.A., 2004. Mineralogy of primary carbonate-bearing hypabyssal kimberlite, Lac de Gras, Slave Province, Northwest Territories, Canada. Lithos 76, 415–433.

Arndt, N.T., Guitreau, M., Boullier, A.M., Le Roex, A., Tommasi, A., Cordier, P., Sobolev, A., 2010. Olivine, and the origin of kimberlite. J. Petrol. 51, 573–602.

Bailey, D.K., 1980. Volatile flux, geotherms, and the generation of the kimberlite-carbonatite-alkaline magma spectrum. Mineral. Mag. 43, 695–699.

Bailey, D.K., 1984. Kimberlite: "The mantle sample" formed by ultrametasomatism. In: Kornprobst, J. (Ed.), Kimberlites: The Mantle and Crust–Mantle Relationships, pp. 323–333.

Barrett, D.R., 1975. The genesis of kimberlites and associated rocks: strontium isotopic evidence. Phys. Chem. Earth 9, 637–653.

Beard, A.D., Downes, H., Hegner, E., Sablukov, S.M., 2000. Geochemistry and mineralogy of kimberlites from the Arkhangelsk Region, NW Russia: evidence for transitional kimberlite magma types. Lithos 51, 47–73.

Boctor, N.Z., Boyd, F.R., 1982. Petrology of kimberlite from the DeBruyn and Martin Mine, Bellsbank, South Africa. Am. Mineral. 67, 917–925.

Boyd, F.R., Clement, C.R., 1977. Compositional zoning of olivines in kimberlites from the De Beers mine, Kimberley, South Africa 76. Carnegie Institution of Washington Yearbook, pp. 485–493.

Brett, R.C., Russell, J.K., Moss, S., 2009. Origin of olivine in kimberlite: phenocryst or impostor? Lithos 112, 201–212.

Brooker, R.A., Sparks, R.S.J., Kavanagh, J.L., Field, M., 2011. The volatile content of hypabyssal kimberlite magmas: some constraints from experiments on natural rock compositions. Bull. Volcanol. 73, 959–981.

Burgess, R., Turner, G., Harris, J.W., 1992. ^{40}Ar–^{39}Ar laser probe studies of clinopyroxene inclusions in eclogitic diamonds. Geochim. Cosmochim. Acta 56, 389–402.

Carlson, R.W., Czamanske, G., Fedorenko, V., Ilupin, I., 2006. A comparison of Siberian meimechites and kimberlites: implications for the source of high-Mg alkalic magmas and flood basalts. Geochem. Geophys. Geosyst. 7.

Cartigny, P., 2005. Stable isotopes and the origin of diamond. Elements 1, 79–84.

Chakhmouradian, A.R., Mitchell, R.H., 2000. Occurrence, alteration patterns and compositional variation of perovskite in kimberlites. Can. Mineral. 38, 975–994.

Chakhmouradian, A.R., Mitchell, R.H., 2001. Three compositional varieties of perovskite from kimberlites of the Lac de Gras field (Northwest Territories, Canada). Mineral. Mag. 65, 133–148.

Chakhmouradian, A., Böhm, C.O., Greville, J.K., 2006. Igneous carbonate-rich rocks from the south Wekusko Lake area, Manitoba (parts of NTS 63 K9 and 63 J12): a kimberlite–carbonatite dilemma. Report of Activities 2006, Manitoba Science, Technology, Energy and Mines, Manitoba Geological Survey.

Chakhmouradian, A.R., Reguir, E.P., Kamenetsky, V.S., Sharygin, V.V., Golovin, A.V., 2013. Trace-element partitioning in perovskite: implications for the geochemistry of kimberlites and other mantle-derived undersaturated rocks. Chem. Geol. http://dx.doi.org/10.1016/j.chemgeo.2013.01.007.

Clarke, D.B., Mitchell, R.H., 1975. Mineralogy and petrology of the kimberlite from Somerset Island, N.W.T. Canada. Phys. Chem. Earth 9, 123–135.

Clarke, D.B., Mitchell, R.H., Chapman, C.A.T., MacKay, R.M., 1994. Occurrence and origin of djerfisherite from the Elwin Bay kimberlite, Somerset Island, Northwest Territories. Can. Mineral. 32, 815–823.

Clement, C.R., 1975. The emplacement of some diatreme-facies kimberlites. Phys. Chem. Earth 9, 51–59.

Clement, C.R., Skinner, E.M.W., 1985. A textural-genetic classification of kimberlites. Trans. Geol. Soc. S. Afr. 88, 403–409.

Clement, C.R., Skinner, E.M.W., Scott Smith, B.H., 1984. Kimberlite re-defined. J. Geol. 32, 223–228.

Cooper, A.F., Gittins, J., 1974. Shortite in kimberlite from Upper Canada Gold Mine, Ontario — discussion. J. Geol. 82, 667–669.

Dalton, J.A., Wood, B.J., 1993. The compositions of primary carbonate melts and their evolution through wallrock reaction in the mantle. Earth Planet. Sci. Lett. 119, 511–525.

Dasgupta, R., Hirschmann, M.M., Dellas, N., 2005. The effect of bulk composition on the solidus of carbonated eclogite from partial melting experiments at 3 GPa. Contributions to. Mineral. Petrol. 149, 288–305.

Dawson, J.B., Hawthorne, J.B., 1973. Magmatic sedimentation and carbonatitic differentiation in kimberlite sills at Benfontein, South Africa. J. Geol. Soc. Lond. 129, 61–85.

Dawson, J., Hill, P., Kinny, P., 2001. Mineral chemistry of a zircon-bearing, composite, veined and metasomatised upper-mantle peridotite xenolith from kimberlite. Contributions to. Mineral. Petrol. 140, 720–733.

Deans, T., Roberts, B., 1984. Carbonatite tuffs and lava clasts of the Tinderet foothills, western Kenya: a study of calcified natrocarbonatites. J. Geol. Soc. Lond. 141, 563–580.

Deines, P., 1989. Stable isotope variations in carbonatites. In: Bell, K. (Ed.), Carbonatites. Genesis and Evolution. Unwin Hyman, London, pp. 301–359.

Deines, P., Gold, D.P., 1973. The isotopic composition of carbonatite and kimberlite carbonates and their bearing on the isotopic composition of deep-seated carbon. Geochim. Cosmochim. Acta 37, 1709–1733.

Distler, V.V., Ilupin, I.P., Laputina, I.P., 1987. Sulfides of deep-seated origin in kimberlites and some aspects of copper–nickel mineralisation. Int. Geol. Rev. 29, 456–464.

Dobrovol'skaya, M.G., Tsepin, A.I., Ilupin, I.P., Ponomarenko, A.I., 1975. Djerfisherite from the kimberlites of Yakutia. In: Tatarinov, P.M. (Ed.), Paragenesis of Minerals in Magmatic Deposits. Nauka, Leningrad, Russia, pp. 3–11.

Doucet, L.S., Ionov, D.A., Golovin, A.V., Pokhilenko, N.P., 2012. Depth, degrees and tectonic settings of mantle melting during craton formation: inferences from major and trace element compositions of spinel harzburgite xenoliths from the Udachnaya kimberlite, central Siberia. Earth Planet. Sci. Lett. 359, 206–218.

Doucet, L.S., Ionov, D.A., Golovin, A.V., 2013. The origin of coarse garnet peridotites in cratonic lithosphere: new data on xenoliths from the Udachnaya kimberlite, central Siberia. Contributions to. Mineral. Petrol. 165, 1225–1242.

Drozdov, A.V., Sukhov, S.S., 2008. A variety of natural systems of industrial groundwater on Siberian platform. Water Resour. 35, 264–273.

Drozdov, A.V., Egorov, K.N., Gotovtsev, S.P., Klimovsky, I.V., 1989. Hydrogeological structure and hydrochemical zonation of the Udachnaya kimberlite pipe. In: Anisimova, N.P. (Ed.), Combined Permafrost and Hydrogeological Studies. Institute of Permafrost Siberian Branch of Academy of Sciences, Yakutsk, pp. 146–155.

Drozdov, A.V., Iost, N.A., Lobanov, V.V., 2008. Cryogeology of the Diamond Deposits in Western Yakutia. Irkutsk State Technical University, Irkutsk (507 pp.).

Edwards, C.B., Howkins, J.B., 1966. Kimberlites in Tanganyika with special reference to Mwadui occurrence. Econ. Geol. 61, 537–554.

Egorov, K.N., 1986. Variation of the isotopic composition of carbon and oxygen during the metasomatic transformation of kimberlites. Dokl. Akad. Nauk SSSR 286, 429–433.

Egorov, K.N., Kornilova, V.P., Safronov, A.F., Filippov, N.D., 1986. Micaceous kimberlite from the Udachnaya-East pipe. Dokl. Akad. Nauk SSSR 291, 199–202.

Egorov, K.N., Ushchapovskaia, Z.F., Kashaev, A.A., Bogdanov, G.V., Sizykh, I.I., 1988. Zemkorite — a new carbonate from Yakutian kimberlites. Dokl. Akad. Nauk SSSR 301, 188–192.

Egorov, K.N., Bogdanov, G.V., Lashkevich, V.V., Medvedeva, T.I., Tikhonova, G.A., 1991. Generations and physical–chemical conditions of serpentinization in kimberlite. Proc. Russ. Mineral. Soc. 120, 1–12.

Egorov, K.N., Solov'eva, L.V., Simakin, S.G., 2004. Megacrystalline cataclastic lherzolite from the Udachnaya Pipe: Mineralogy, geochemistry, and genesis. Dokl. Earth Sci. 397, 698–702.

Emeleus, C.H., Andrews, J.R., 1975. Mineralogy and petrology of kimberlite dyke and sheet intrusions and included peridotite xenoliths from South West Greenland. Phys. Chem. Earth 9, 179–198.

Exley, R.A., Jones, A.P., 1983. $^{87}Sr/^{86}Sr$ in kimberlitic carbonates by ion microprobe: hydrothermal alteration, crustal contamination and relation to carbonatite. Contrib. Mineral. Petrol. 83, 288–292.

Fedortchouk, Y., Canil, D., 2004. Intensive variables in kimberlite magmas, Lac de Gras, Canada and implications for diamond survival. J. Petrol. 45, 1725–1745.

Fontana, G., Mac Niocaill, C., Brown, R.J., Sparks, R.S.J., Field, M., 2011. Emplacement temperatures of pyroclastic and volcaniclastic deposits in kimberlite pipes in southern Africa. Bull. Volcanol. 73, 1063–1083.

Fraser, K.J., Hawkesworth, C.J., Erlank, A.J., Mitchel, R.H., Scott-Smith, B.H., 1985. Sr, Nd, and Pb isotope and minor element geochemistry of lamproites and kimberlites. Earth Planet. Sci. Lett. 76, 57–70.

Frezzotti, M.L., Andersen, T., Neumann, E.R., Simonsen, S.L., 2002. Carbonatite melt–CO_2 fluid inclusions in mantle xenoliths from Tenerife, Canary Islands: a story of trapping, immiscibility and fluid–rock interaction in the upper mantle. Lithos 64, 77–96.

Frezzotti, M.L., Ferrando, S., Peccerillo, A., Petrelli, M., Tecce, F., Perucchi, A., 2010. Chlorine-rich metasomatic H_2O–CO_2 fluids in amphibole-bearing peridotites from Injibara (Lake Tana region, Ethiopian plateau): nature and evolution of volatiles in the mantle of a region of continental flood basalts. Geochim. Cosmochim. Acta 74, 3023–3039.

Giuliani, A., Kamenetsky, V.S., Phillips, D., Kendrick, M.A., Wyatt, B.A., Goemann, K., 2012. Nature of alkali-carbonate fluids in the sub-continental lithospheric mantle. Geology 40, 967–970.

Giuliani, A., Kamenetsky, V.S., Kendrick, M.A., Phillips, D., Goemann, K., 2013a. Nickel-rich metasomatism of the lithospheric mantle by pre-kimberlitic alkali-S–Cl-rich C–O–H fluids. Contrib. Mineral. Petrol. 165, 155–171.

Giuliani, A., Kamenetsky, V.S., Kendrick, M.A., Phillips, D., Wyatt, B.A., Maas, R., 2013b. Oxide, sulphide and carbonate minerals in a mantle polymict breccia: metasomatism by proto-kimberlite magmas, and relationship to the kimberlite megacrystic suite. Chem. Geol. 353, 4–18.

Giuliani, A., Phillips, D., Kamenetsky, V.S., Fiorentini, M.L., Farquhar, J., Kendrick, M.A., 2014. Stable isotope (C, O, S) compositions of volatile-rich minerals in kimberlites: a review. Chem. Geol. 374–375, 61–83.

Golovin, A.V., Sharygin, V.V., Pokhilenko, N.P., Mal'kovets, V.G., Kolesov, B.A., Sobolev, N.V., 2003. Secondary melt inclusions in olivine from unaltered kimberlites of the Udachnaya-East pipe, Yakutia. Dokl. Earth Sci. 388, 93–96.

Golovin, A.V., Sharygin, V.V., Pokhilenko, N.P., 2007. Melt inclusions in olivine phenocrysts in unaltered kimberlites from the Udachnaya-East pipe, Yakutia: some aspects of kimberlite magma evolution during late crystallization stages. Petrology 15, 168–183.

Green, D.H., Wallace, M.E., 1988. Mantle metasomatism by ephemeral carbonatite melts. Nature 336, 459–462.

Heaman, L.M., 1989. The nature of the subcontinental mantle from Sr–Nd–Pb isotopic studies on kimberlitic perovskite. Earth Planet. Sci. Lett. 92, 323–334.

Holser, W.T., 1979. Trace elements and isotopes in evaporites. In: Bums, R.G. (Ed.), Marine Minerals. Mineralogical Society of America, Washington D. C., pp. 295–346.

Howard, C.L.H., Kerr, P.F., 1960. Blue halite. Science 132, 1886–1887.

Ito, M., 1986. Kimberlites and their ultramafic xenoliths from western Kenya. Tschermaks Mineral. Petrogr. Mitt. 35 (3), 193–216.

Izraeli, E.S., Harris, J.W., Navon, O., 2001. Brine inclusions in diamonds: a new upper mantle fluid. Earth Planet. Sci. Lett. 187, 323–332.

Kamenetsky, V.S., Kamenetsky, M.B., 2010. Magmatic fluids immiscible with silicate melts: examples from inclusions in phenocrysts and glasses, and implications for magma evolution and metal transport. Geofluids 10, 293–311.

Kamenetsky, V.S., Crawford, A.J., Meffre, S., 2001. Factors controlling chemistry of magmatic spinel: an empirical study of associated olivine, Cr-spinel and melt inclusions from primitive rocks. J. Petrol. 42, 655–671.

Kamenetsky, M.B., Sobolev, A.V., Kamenetsky, V.S., Maas, R., Danyushevsky, L.V., Thomas, R., Sobolev, N.V., Pokhilenko, N.P., 2004. Kimberlite melts rich in alkali chlorides and carbonates: a potent metasomatic agent in the mantle. Geology 32, 845–848.

Kamenetsky, V.S., Sharygin, V.V., Kamenetsky, M.B., Golovin, A.V., 2006. Chloride–carbonate nodules in kimberlites from the Udachnaya pipe: alternative approach to the evolution of kimberlite magmas. Geochem. Int. 44, 935–940.

Kamenetsky, V.S., Kamenetsky, M.B., Sharygin, V.V., Faure, K., Golovin, A.V., 2007a. Chloride and carbonate immiscible liquids at the closure of the kimberlite magma evolution (Udachnaya-East kimberlite, Siberia). Chem. Geol. 237, 384–400.

Kamenetsky, V.S., Kamenetsky, M.B., Sharygin, V.V., Golovin, A.V., 2007b. Carbonate-chloride enrichment in fresh kimberlites of the Udachnaya-East pipe, Siberia: a clue to physical properties of kimberlite magmas? Geophys. Res. Lett. 34, L09316. http://dx.doi.org/10.1029/2007GL029389.

Kamenetsky, V.S., Kamenetsky, M.B., Sobolev, A.V., Golovin, A.V., Demouchy, S., Faure, K., Sharygin, V.V., Kuzmin, D.V., 2008. Olivine in the Udachnaya-East kimberlite (Yakutia, Russia): types, compositions and origins. J. Petrol. 49, 823–839.

Kamenetsky, V.S., Kamenetsky, M.B., Sobolev, A.V., Golovin, A.V., Sharygin, V.V., Pokhilenko, N.P., Sobolev, N.V., 2009a. Can pyroxenes be liquidus minerals in the kimberlite magma? Lithos 112, 213–222.

Kamenetsky, V.S., Kamenetsky, M.B., Weiss, Y., Navon, O., Nielsen, T.F.D., Mernagh, T.P., 2009b. How unique is the Udachnaya-East kimberlite? Comparison with kimberlites from the Slave Craton (Canada) and SW Greenland. Lithos 112, 334–346.

Kamenetsky, V.S., Maas, R., Kamenetsky, M.B., Paton, C., Phillips, D., Golovin, A.V., Gornova, M.A., 2009c. Chlorine from the mantle: magmatic halides in the Udachnaya-East kimberlite, Siberia. Earth Planet. Sci. Lett. 285, 96–104.

Kamenetsky, V.S., Chung, S.-L., Kamenetsky, M.B., Kuzmin, D.V., 2012a. Picrites from the Emeishan Large Igneous Province, SW China: a compositional continuum in primitive magmas and respective mantle sources. J. Petrol. 53, 2095–2113.

Kamenetsky, V.S., Kamenetsky, M.B., Golovin, A.V., Sharygin, V.V., Maas, R., 2012b. Ultrafresh salty kimberlite of the Udachnaya–East pipe (Yakutia, Russia): a petrological oddity or fortuitous discovery? Lithos 152, 173–186.

Kamenetsky, V.S., Grütter, H., Kamenetsky, M.B., Gömann, K., 2013. Parental carbonatitic melt of the Koala kimberlite (Canada): constraints from melt inclusions in olivine and Cr-spinel, and groundmass carbonate. Chem. Geol. 353, 96–111.

Kamenetsky, V.S., Belousova, E.A., Giuliani, A., Kamenetsky, M.B., Goemann, K., Griffin, W.L., 2014. Chemical abrasion of zircon and ilmenite megacrysts in the Monastery kimberlite: implications for the composition of kimberlite melts. Chem. Geol. 383, 76–85.

Keller, J., Hoefs, J., 1995. Stable isotope characteristics of recent natrocarbonatites from Oldoinyo Lengai. In: Bell, K., Keller, J. (Eds.), Carbonatite volcanism: Oldoinyo Lengai and petrogenesis of natrocarbonatites. Springer-Verlag, pp. 113–123.

Keller, J., Zaitsev, A.N., 2006. Calciocarbonatite dykes at Oldoinyo Lengai, Tanzania: the fate of natrocarbonatite. Can. Mineral. 44, 857–876.

Kharkiv, A.D., Zuenko, V.V., Zinchuk, N.N., Kryuchkov, A.I., Ukhanov, A.V., Bogatykh, M.M., 1991. Petrochemistry of kimberlites. Nedra, Moscow (304 pp.).

Kinny, P.D., Griffin, W.L., Heaman, L.M., Brakhfogel, F.F., Spetsius, Z.V., 1997. SHRIMP U–Pb ages of perovskite from Yakutian kimberlites. Russ. Geol. Geophys. 38, 91–99.

Kirkley, M.B., Smith, H.S., Gurney, J.J., 1989. Kimberlite carbonates — a carbon and oxygen stable isotope study. In: Ross, J., et al. (Eds.), Kimberlites and related rocks: their composition, occurrence, origin and emplacement. Blackwell Scientific Publications, Sydney, pp. 264–281.

Kjarsgaard, B.A., Pearson, D.G., Tappe, S., Nowell, G.M., Dowall, D.P., 2009. Geochemistry of hypabyssal kimberlites from Lac de Gras, Canada: comparisons to a global database and applications to the parent magma problem. Lithos 112, 236–248.

Klein-BenDavid, O., Izraeli, E.S., Hauri, E., Navon, O., 2007a. Fluid inclusions in diamonds from the Diavik mine, Canada and the evolution of diamond-forming fluids. Geochim. Cosmochim. Acta 71, 723–744.

Klein-BenDavid, O., Wirth, R., Navon, O., 2007b. Micrometer-scale cavities in fibrous and cloudy diamonds — a glance into diamond dissolution events. Earth Planet. Sci. Lett. 264, 89–103.

Klein-BenDavid, O., Logvinova, A.M., Schrauder, M., Spetius, Z.V., Weiss, Y., Hauri, E.H., Kaminsky, F.V., Sobolev, N.V., 2009. High-Mg carbonatitic microinclusions in some Yakutian diamonds — a new type of diamond-forming fluid. Lithos 112, 648–659.

Kobelski, B.J., Gold, D.P., Deines, P., 1979. Variations in stable isotope compositions for carbon and oxygen in some South African and Lesothan kimberlites. In: Boyd, F.R., Meyer, H.O.A. (Eds.), Kimberlites, Diatremes and Diamonds: Their Geology, Petrology, and Geochemistry. American Geophysical Union, Washington DC, pp. 252–271.

Kogarko, L.N., Ryabchikov, I.D., 2000. Geochemical evidence for meimechite magma generation in the subcontinental lithosphere of Polar Siberia. J. Asian Earth Sci. 18, 195–203.

Konzett, J., Armstrong, R.A., Günther, D., 2000. Modal metasomatism in the Kaapvaal craton lithosphere: constraints on timing and genesis from U–Pb zircon dating of metasomatized peridotites and MARID-type xenoliths. Contrib. Mineral. Petrol. 139, 704–719.

Kopylova, M.G., Hayman, P., 2008. Petrology and textural classification of the Jericho kimberlite, northern Slave Province, Nunavut, Canada. Can. J. Earth Sci. 45, 701–723.

Kopylova, M.G., Kostrovitsky, S.I., Egorov, K.N., 2013. Salts in southern Yakutian kimberlites and the problem of primary alkali kimberlite melts. Earth Sci. Rev. 119, 1–16.

Kornilova, V.P., Marshintsev, V.K., Novoselov, Y.M., 1981. Shortite in the Udachnaya-East kimberlites. Bull. Sci. Tech. Inf. 7, 19–21.

Kostrovitsky, S.I., Morikiyo, T., Serov, I.V., Yakovlev, D.A., Amirzhanov, A.A., 2007. Isotope-geochemical systematics of kimberlites and related rocks from the Siberian Platform. Russ. Geol. Geophys. 48, 272–290.

Kostrovitsky, S.I., Kopylova, M.G., Egorov, K.N., Yakovlev, D.A., 2013. The "exceptionally fresh" Udachnaya-East kimberlite: evidence for brine and evaporite contamination. In: Pearson, D.G., et al. (Eds.), Proceedings of the 10th International Kimberlite Conference, pp. 75–91.

Kruger, F.J., 1982. The occurrence of cebollite in kimberlite and included zeolitized crustal xenoliths — a correction and discussion of the occurrence of pectolite. Mineral. Mag. 46, 274–275.

le Roex, A.P., Bell, D.R., Davis, P., 2003. Petrogenesis of group I kimberlites from Kimberley, South Africa: evidence from bulk-rock geochemistry. J. Petrol. 44, 2261–2286.

Litasov, K.D., Ohtani, E., 2009. Phase relations in the peridotite-carbonate-chloride system at 7.0–16.5 GPa and the role of chlorides in the origin of kimberlite and diamond. Chem. Geol. 262, 29–41.

Litasov, K.D., Shatskiy, A., Ohtani, E., Yaxley, G.M., 2013. Solidus of alkaline carbonatite in the deep mantle. Geology 41 (1), 79–82.

Maas, R., Kamenetsky, M.B., Sobolev, A.V., Kamenetsky, V.S., Sobolev, N.V., 2005. Sr, Nd, and Pb isotope evidence for a mantle origin of alkali chlorides and carbonates in the Udachnaya kimberlite, Siberia. Geology 33 (7), 549–552.

Marshintsev, V.K., 1986. Vertical heterogeneity of kimberlite bodies in Yakutiya. Nauka, Novosibirsk (239 pp.).

Marshintsev, V.K., Migalkin, K.N., Nikolaev, N.C., Barashkov, Y.P., 1976. Unaltered kimberlite of the Udachnaya East pipe. Transactions (Doklady) of the USSR Academy of Sciences 231, pp. 961–964.

Maslovskaja, M.N., Yegorov, K.N., Kolosnitsyna, T.I., Brandt, S.B., 1983. Strontium isotope composition, Rb–Sr absolute age, and rare alkalies in micas from Yakutian kimberlites. Dokl. Akad. Nauk SSSR 266 (2), 451–455.

Mernagh, T.P., Kamenetsky, V.S., Kamenetsky, M.B., 2011. A Raman microprobe study of melt Inclusions in kimberlites from Siberia, Canada, SW Greenland and South Africa. Spectrochim. Acta A Mol. Biomol. Spectrosc. 80A (1), 82–87.

Meyer, H.O.A., 1976. Kimberlites of the continental United States: a review. J. Geol. 84 (4), 377–403.

Misra, K.C., Anand, M., Taylor, L.A., Sobolev, N.V., 2004. Multi-stage metasomatism of diamondiferous eclogite xenoliths from the Udachnaya kimberlite pipe, Yakutia, Siberia. Contrib. Mineral. Petrol. 146 (6), 696–714.

Mitchell, R.H., 1973. Composition of olivine, silica activity and oxygen fugacity in kimberlite. Lithos 6, 65–81.

Mitchell, R.H., 1978. Mineralogy of the Elwin Bay kimberlite, Somerset Island, N.W.T., Canada. Am. Mineral. 63, 47–57.

Mitchell, R.H., 1984. Mineralogy and origin of carbonate-rich segregations in a composite kimberlite sill. Neues Jahrb. Mineral. Abh. 150, 185–197.

Mitchell, R.H., 1986. Kimberlites: Mineralogy, Geochemistry and Petrology. Plenum Press, New York (442 pp.).

Mitchell, R.H., 1995. Kimberlites, Orangeites and Related Rocks. Plenium Press, New York (410 pp.).

Mitchell, R.H., 1997. Carbonate-carbonate immiscibility, neighborite and potassium iron sulphide in Oldoinyo Lengai natrocarbonatite. Mineral. Mag. 61, 779–789.

Mitchell, R.H., 2006. Sylvite and fluorite microcrysts, and fluorite-nyerereite intergrowths from natrocarbonatite, Oldoinyo Lengai, Tanzania. Mineral. Mag. 70 (1), 103–114.

Mitchell, R.H., 2008. Petrology of hypabyssal kimberlites: relevance to primary magma compositions. J. Volcanol. Geotherm. Res. 174, 1–8.

Mitchell, R.H., Kjarsgaard, B.A., 2008. Experimental studies of the system $Na_2Ca(CO_3)_2$–NaCl–KCl at 0.1 GPa: implications for the differentiation and low-temperature crystallization of natrocarbonatite. Can. Mineral. 46, 971–980.

Mitchell, R.H., Skinner, E.M.W., Smith, B.H.S., 2009. Tuffisitic kimberlites from the Wesselton Mine, South Africa: mineralogical characteristics relevant to their formation. Lithos 112, 452–464.

Moss, S., Russell, J.K., 2011. Fragmentation in kimberlite: products and intensity of explosive eruption. Bull. Volcanol. 73 (8), 983–1003.

Moss, S., Russell, J.K., Andrews, G.D.M., 2008. Progressive infilling of a kimberlite pipe at Diavik, Northwest Territories, Canada: insights from volcanic facies architecture, textures, and granulometry. J. Volcanol. Geotherm. Res. 174 (1–3), 103–116.

Moss, S., Russell, J.K., Brett, R.C., Andrews, G.D.M., 2009. Spatial and temporal evolution of kimberlite magma at A154N, Diavik, Northwest Territories, Canada. Lithos 112, 541–552.

Navon, O., Hutcheon, I.D., Rossman, G.R., Wasserburg, G.J., 1988. Mantle-derived fluids in diamond micro-inclusions. Nature 335, 784–789.

Nielsen, T.F.D., Jensen, S.M., 2005. The Majuagaa calcite-kimberlite dyke, Maniitsoq, southern West Greenland. Geological Survey of Denmark and Greenland, Report 2005/43.

Nowell, G.M., Pearson, D.G., Bell, D.R., Carlson, R.W., Smith, C.B., Kempton, P.D., Noble, S.R., 2004. Hf isotope systematics of kimberlites and their megacrysts: new constraints on their source regions. J. Petrol. 45 (8), 1583–1612.

Nowicki, T., Porritt, L., Crawford, B., Kjarsgaard, B., 2008. Geochemical trends in kimberlites of the Ekati property, Northwest Territories, Canada: insights on volcanic and resedimentation processes. J. Volcanol. Geotherm. Res. 174 (1–3), 117–127.

Onuma, N., Ninomiya, S., Nagasawa, H., 1981. Mineral/groundmass partition coefficients for nepheline, melilite, clinopyroxene and perovskite in melilite-nepheline basalt, Nyiragongo, Zaire. Geochem. J. 15 (4), 221–228.

Palyanov, Y.N., Shatsky, V.S., Sobolev, N.V., Sokol, A.G., 2007. The role of mantle ultrapotassic fluids in diamond formation. Proc. Natl. Acad. Sci. U. S. A. 104 (22), 9122–9127.

Pal'yanov, Y.N., Sokol, A.G., Borzdov, Y.M., Khokhryakov, A.F., Sobolev, N.V., 1999. Diamond formation from mantle carbonate fluids. Nature 400, 417–418.

Pal'yanov, Y.N., Sokol, A.G., Borzdov, Y.M., Khokhryakov, A.F., 2002. Fluid-bearing alkaline carbonate melts as the medium for the formation of diamonds in the Earth's mantle: an experimental study. Lithos 60, 145–159.

Parthasarathy, G., Chetty, T.R.K., Haggerty, S.E., 2002. Thermal stability and spectroscopic studies of zemkorite: a carbonate from the Venkatampalle kimberlite of southern India. Am. Mineral. 87 (10), 1384–1389.

Paton, C., Hergt, J.M., Phillips, D., Woodhead, J.D., Shee, S.R., 2007. New insights into the genesis of Indian kimberlites from the Dharwar Craton via in situ Sr isotope analysis of groundmass perovskite. Geology 35 (11), 1011–1014.

Patterson, M., Francis, D., McCandless, T., 2009. Kimberlites: magmas or mixtures? Lithos 112, 191–200.

Pavlov, D.I., Ilupin, I.P., Gorbacheva, S.A., 1985. Connate brines of the Siberian Platform as a factor in the alteration of kimberlite. Int. Geol. Rev. 27 (5), 600–610.

Pilbeam, L.H., Nielsen, T.F.D., Waight, T.E., 2013. Digestion Fractional Crystallization (DFC): an important process in the genesis of kimberlites. Evidence from olivine in the Majuagaa kimberlite, southern west Greenland. J. Petrol. 54, 1399–1425.

Plyusnin, G.S., Samoylov, V.S., Golyshev, S.I., 1980. Use of $\delta^{13}C$-$\delta^{18}O$ isotope pairs and carbonatite temperature facies. Dokl. Akad. Nauk SSSR 254 (5), 1241–1245.

Pokhilenko, L.N., Golovin, A.V., Sharygin, I.S., Pokhilenko, N.P., 2011. Accessory minerals of mantle xenoliths: first finds of Cl-free K-Fe sulfides. Dokl. Earth Sci. 440 (2), 1404–1409.

Price, S.E., Russell, J.K., Kopylova, M.G., 2000. Primitive magma from the Jericho Pipe, NWT, Canada: constraints on primary kimberlite melt chemistry. J. Petrol. 41 (6), 789–808.

Putirka, K., 1999. Melting depths and mantle heterogeneity beneath Hawaii and the East Pacific Rise: constraints from Na/Ti and rare earth element ratios. J. Geophys. Res. Solid Earth 104 (B2), 2817–2829.

Raber, E., Haggerty, S.E., 1979. Zircon-oxide reactions in diamond-bearing kimberlites. In: Boyd, F.R., Meyer, H.O.A. (Eds.), 2nd International Kimberlite Conference. American Geophysical Union, Washington, DC, pp. 229–239.

Rao, N.V.C., Gibson, S.A., Pyle, D.M., Dickin, A.P., 2004. Petrogenesis of Proterozoic lamproites and kimberlites from the Cuddapah basin and Dharwar Craton, Southern India. J. Petrol. 45 (2), 907–948.

Safonov, O.G., Perchuk, L.L., Litvin, Y.A., 2007. Melting relations in the chloride–carbonate–silicate systems at high-pressure and the model for formation of alkalic diamond–forming liquids in the upper mantle. Earth Planet. Sci. Lett. 253, 112–128.

Safonov, O.G., Kamenetsky, V.S., Perchuk, L.L., 2011. Links between carbonatite and kimberlite melts in chloride–carbonate–silicate systems: experiments and application to natural assemblages. J. Petrol. 52, 1307–1331.

Schrauder, M., Navon, O., 1994. Hydrous and carbonatitic mantle fluids in fibrous diamonds from Jwaneng, Botswana. Geochim. Cosmochim. Acta 58 (2), 761–771.

Scott Smith, B.H., Skinner, E.M., Clement, C.R., 1983. Further data on the occurrence of pectolite in kimberlite. Mineral. Mag. 47 (342), 75–78.

Sharp, Z.D., Barnes, J.D., Brearley, A.J., Fischer, T., Chaussidon, M., Kamenetsky, V.S., 2007. Chlorine isotope homogeneity of the mantle, crust and carbonaceous chondrites. Nature 446, 1062–1065.

Sharp, Z.D., Mercer, J.A., Jones, R.H., Brearley, A.J., Selverstone, J., Bekker, A., Stachel, T., 2013. The chlorine isotope composition of chondrites and Earth. Geochim. Cosmochim. Acta 189–204.

Sharygin, I.S., Golovin, A.V., 2011. Djerfisherite in kimberlites of the Kuoikskoe field as an indicator of enrichment of kimberlite melts in chlorine. Dokl. Earth Sci. 436 (2), 301–307.

Sharygin, V.V., Golovin, A.V., Pokhilenko, N.P., Sobolev, N.V., 2003. Djerfisherite in unaltered kimberlites of the Udachnaya-East pipe, Yakutia. Dokl. Earth Sci. 390 (4), 554–557.

Sharygin, V.V., Golovin, A.V., Pokhilenko, N.P., Kamenetsky, V.S., 2007. Djerfisherite in the Udachnaya-East pipe kimberlites (Sakha-Yakutia, Russia): paragenesis, composition and origin. Eur. J. Mineral. 19 (1), 51–63.

Sharygin, V.V., Kamenetsky, V.S., Kamenetsky, M.B., 2008. Potassium sulfides in kimberlite-hosted chloride-"nyerereite" and chloride clasts of Udachnaya-East pipe, Yakutia, Russia. Can. Mineral. 46 (Part 4), 1079–1095.

Sharygin, I.S., Golovin, A.V., Pokhilenko, N.P., 2012. Djerfisherite in xenoliths of sheared peridotite in the Udachnaya-East pipe (Yakutia): origin and relationship with kimberlitic magmatism. Russ. Geol. Geophys. 53 (3), 247–261.

Shatsky, V., Ragozin, A., Zedgenizov, D., Mityukhin, S., 2008. Evidence for multistage evolution in a xenolith of diamond-bearing eclogite from the Udachnaya kimberlite pipe. Lithos 105 (3–4), 289–300.

Shee, S.R., 1985. The petrogenesis of the Wesselton mine kimberlites, Kimberley, Cape Province, R.S.A.(PhD Thesis) University of Cape Town.

Shirey, S.B., Cartigny, P., Frost, D.J., Keshav, S., Nestola, F., Nimis, P., Pearson, D.G., Sobolev, N.V., Walter, M.J., 2013. Diamonds and the Geology of Mantle Carbon, Reviews in Mineralogy and Geochemistry. Mineral. Soc. Am. 355–421.

Shiryaev, A.A., Izraeli, E.S., Hauri, E.H., Zakharchenko, O.D., Navon, O., 2005. Chemical, optical and isotopic investigation of fibrous diamonds from Brazil. Russ. Geol. Geophys. 46 (12), 1185–1201.

Smith, C.B., 1983. Pb, Sr and Nd isotopic evidence for sources of southern African Cretaceous kimberlites. Nature 304, 51–54.

Smith, C.B., Gurney, J.J., Skinner, E.M.W., Clement, C.R., Ebrahim, N., 1985. Geochemical character of the southern African kimberlites: a new approach based on isotopic constraints. Trans. Geol. Soc. S. Afr. 88, 267–280.

Smith, C.B., Sims, K., Chimuka, L., Duffin, A., Beard, A.D., Townend, R., 2004. Kimberlite metasomatism at Murowa and Sese pipes, Zimbabwe. Lithos 76 (1–4), 219–232.

Smith, E.M., Kopylova, M.G., Dubrovinsky, L., Navon, O., Ryder, J., Tomlinson, E.L., 2011. Transmission X-ray diffraction as a new tool for diamond fluid inclusion studies. Mineral. Mag. 75 (5), 2657–2675.

Smith, E.M., Kopylova, M.G., Nowell, G.M., Pearson, D.G., Ryder, J., 2012. Archean mantle fluids preserved in fibrous diamonds from Wawa, Superior craton. Geology 40 (12), 1071–1074.

Sobolev, A.V., Sobolev, N.V., Smith, C.B., Dubessy, J., 1989. Fluid and melt compositions in lamproites and kimberlites based on the study of inclusions in olivine. In: Ross, J., et al. (Eds.), Kimberlites and Related Rocks: Their Composition, Occurrence, Origin and Emplacement. Blackwell Scientific Publications, Sydney, pp. 220–241.

Sobolev, A.V., Kamenetsky, V.S., Kononkova, N.N., 1992. New data on Siberian meymechite petrology. Geochem. Int. 29 (3), 10–20.

Sobolev, V.N., Taylor, L.A., Snyder, G.A., Jerde, E.A., Neal, C.R., Sobolev, N.V., 1999. Quantifying the effects of metasomatism in mantle xenoliths: constraints from secondary chemistry and mineralogy in Udachnaya eclogites, Yakutia. Int. Geol. Rev. 41 (5), 391–416.

Sobolev, A.V., Krivolutskaya, N.A., Kuzmin, D.V., 2009. Petrology of the parental melts and mantle sources of Siberian trap magmatism. Petrology 17 (3), 253–286.

Solovjeva, L.V., Egorov, K.N., Markova, M.E., Kharkiv, A.D., Popolitov, K.E., Barankevich, V.G., 1997. Mantle metasomatism and melting in mantle-derived xenoliths from the Udachnaya kimberlite; their possible relationship with diamond and kimberlite formation. Russ. Geol. Geophys. 38 (1), 182–204.

Sonnenfeld, P., 1995. The color of rock salt — a review. Sediment. Geol. 94 (3–4), 267–276.

Sparks, R.S.J., Brooker, R.A., Field, M., Kavanagh, J., Schumacher, J.C., Walter, M.J., White, J., 2009. The nature of erupting kimberlite melts. Lithos 112, 429–438.

Spetsius, Z.V., Taylor, L.A., 2002. Partial melting in mantle eclogite xenoliths: connections with diamond paragenesis. Int. Geol. Rev. 44, 973–987.

Spetsius, Z.V., Taylor, L.A., 2008. Diamonds of Yakutia: petrographic evidence for their origin. Tranquility Base Press, Lenoir City, Tennessee, USA (278 pp.).

Spetsius, Z.V., Bulanova, G.P., Leskova, N.V., 1987. Djerfisherite and its genesis in kimberlite rocks. Dokl. Akad. Nauk SSSR 293 (1), 199–202.

Spiridonov, E.M., Pautov, L.A., Sokolova, E.L., Vorob'ev, E.I., Agakhanov, A.A., 2010. Chlorine-bearing lizardite from metakimberlite of the Udachnaya-East pipe, northern Yakutia. Dokl. Earth Sci. 431 (1), 403–405.

Sukhov, S.S., Lobanov, V.V., 2003. Analysis of paleostratigraphy of the Cambrian deposits around the Udachnaya pipe: assessment of the hydrogeological conditions for mine development to depths of proven ore reserves (project # 23-00-76), Mirniy-Novosibirsk.

Taylor, H.P.J., Frechen, J., Degens, E.T., 1967. Oxygen and carbon isotope studies of carbonatites from Laacher See district, West Germany and the Alnö district, Sweden. Geochim. Cosmochim. Acta 31, 407–430.

Thibault, Y., Edgar, A.D., Lloyd, F.E., 1992. Experimental investigation of melts from a carbonated phlogopite lherzolite: implications for metasomatism in the continental lithospheric mantle. Am. Mineral. 77, 784–794.

Tomlinson, E.L., Jones, A.P., Harris, J.W., 2006. Co-existing fluid and silicate inclusions in mantle diamond. Earth Planet. Sci. Lett. 250 (3–4), 581–595.

van Achterbergh, E., Griffin, W.L., Ryan, C.G., O'Reilly, S.Y., Pearson, N.J., Kivi, K., Doyle, B.J., 2002. Subduction signature for quenched carbonatites from the deep lithosphere. Geology 30 (8), 743–746.

Vasilenko, V.B., Zinchuk, N.N., Krasavchikov, V.O., Kuznetsova, L.G., Khlestov, V.V., Volkova, N.I., 2002. Diamond potential estimation based on kimberlite major element chemistry. J. Geochem. Explor. 76, 93–112.

Vinogradov, V.I., Ilupin, I.P., 1972. Isotope composition of sulfur in kimberlite of the Siberian Platform. Dokl. Akad. Nauk 204, 221–223.

Wallace, M.E., Green, D.H., 1988. An experimental determination of primary carbonatite magma composition. Nature 335 (6188), 343–346.

Watkinson, D.H., Chao, G.Y., 1973. Shortite in kimberlite from the Upper Canada Gold Mine, Ontario. J. Geol. 81, 229–233.

Weis, D., Demaiffe, D., 1985. A depleted mantle source for kimberlites from Zaire: Nd, Sr and Pb isotopic evidence. Earth Planet. Sci. Lett. 73, 269–277.

Weiss, Y., 2012. Microinclusions in Diamonds: composition, source and mantle metasomatism(PhD Thesis) The Hebrew University.

Weiss, Y., Griffin, W.L., Elhlou, S., Navon, O., 2008. Comparison between LA-ICP-MS and EPMA analysis of trace elements in diamonds. Chem. Geol. 252 (3–4), 158–168.

Weiss, Y., Kessel, R., Griffin, W.L., Kiflawi, I., Klein-BenDavid, O., Bell, D.R., Harris, J.W., Navon, O., 2009. A new model for the evolution of diamond-forming fluids: evidence from microinclusion-bearing diamonds from Kankan, Guinea. Lithos 112, 660–674.

Weiss, Y., Griffin, W.L., Bell, D.R., Navon, O., 2011. High-Mg carbonatitic melts in diamonds, kimberlites and the sub-continental lithosphere. Earth Planet. Sci. Lett. 309 (3–4), 337–347.

White, J.L., Sparks, R.S.J., Bailey, K., Barnett, W.P., Field, M., Windsor, L., 2012. Kimberlite sills and dykes associated with the Wesselton kimberlite pipe, Kimberley, South Africa. S. Afr. J. Geol. 115 (1), 1–32.

Woodhead, J., Hergt, J., Phillips, D., Paton, C., 2009. African kimberlites revisited: in situ Sr-isotope analysis of groundmass perovskite. Lithos 112, 311–317.

Zaitsev, A.N., Keller, J., 2006. Mineralogical and chemical transformation of Oldoinyo Lengai natrocarbonatites, Tanzania. Lithos 91 (1–4), 191–207.

Zaitsev, A.N., Keller, J., Spratt, J., Perova, E.N., Kearsley, A., 2008. Nyererite–pirssonite–calcite–shortite relationships in altered natrocarbonatites, Oldoinyo Lengai, Tanzania. Can. Mineral. 46, 843–860.

Zaitsev, A.N., Wenzel, T., Vennemann, T., Markl, G., 2013. Tinderet volcano, Kenya: an altered natrocarbonatite locality? Mineral. Mag. 77 (3), 209–222.

Zedgenizov, D.A., Ragozin, A.L., Shatsky, V.S., Araujo, D., Griffin, W.L., Kagi, H., 2009. Mg and Fe-rich carbonate-silicate high-density fluids in cuboid diamonds from the Internationalnaya kimberlite pipe (Yakutia). Lithos 112, 638–647.